



Disentangling environmental drivers of Subarctic dinocyst assemblage compositional change during the Holocene

Sabrina Hohmann¹, Michal Kucera¹, Anne de Vernal²

5

¹ MARUM – Center for Marine Environmental Sciences, University of Bremen, Bremen, Leobener Straße 8, D-28359 Bremen, Germany

² Centre Geotop, Université du Québec à Montréal, Montréal, C.P. 8888, Succ. Centre-Ville, Montréal, QC, H3C 3P8, Canada

10 *Correspondence to:* Sabrina Hohmann (hohmannlls@gmail.de)

Abstract. Analysis of compositional changes in fossil organic-walled dinoflagellate cyst (dinocysts) assemblages is a widely used tool for the quantitative reconstruction of past environmental parameters. This approach assumes that the assemblage composition is significantly and independently related to the reconstructed environmental parameters. Theoretically, dinocyst assemblages can be used to reconstruct multiple environmental variables. However, there is evidence that primary and subordinate drivers for assemblage compositions differ regionally and it remains unclear whether a significant relationship to specific parameters in the present ocean always implies that this relationship is significant in fossil assemblages, questioning if past changes in these multiple parameters can be reconstructed simultaneously from fossil assemblages. Here, we analysed a local subset of the Northern Hemisphere dinocyst calibration dataset (n = 1968), including samples from the Baffin Bay area (n = 421), and evaluated the benefits of a local versus a more regional or global calibration for the environmental reconstruction of Baffin Bay oceanography during the Holocene. We determined the dimensionality of the dinocyst ecological response and identified environmental drivers in the Baffin Bay area for the modern dataset. We analysed four existing Holocene records along a North-South transect in the area and evaluated the statistical significance of downcore reconstructions by applying the local and global datasets with different techniques: the modern analogue technique (MAT), the weighted average partial least square (WA-PLS), and maximum likelihood (ML). We evaluate reconstructions tested as significant in the light of the existing state of knowledge about West Greenland's Holocene paleoceanography. Our analyses imply that present-day and Holocene dinocyst assemblages in the Baffin Bay area are primarily driven by salinity changes; other parameters were less important in driving assemblage compositions and their contribution differed among the studied records. We show that the objectively occurring and temporally coherent shifts in dinocyst assemblages in the Holocene of Baffin Bay can be interpreted robustly only by transfer functions that are calibrated locally. Transfer functions based on the broad North Hemisphere calibration yielded many insignificant environmental reconstructions. At the same time, we show that even in the local calibration, not all parameters that appear to significantly affect dinocyst assemblages in the calibration dataset can be meaningfully reconstructed



in the fossil record. A thorough evaluation of the calibration dataset and the significance of downcore applications is necessary
35 to reveal the region-specific information contained in dinocyst assemblage composition.

1 Introduction

During the last decades, the growing interest in environmental responses to changing climate produced many studies
40 documenting climate variations based on reconstructions making use of marine microfossils (Muller et al., 1983; Sarnthein et
al., 1988; Berger et al., 1989; Meyers, 1997; Rühlemann et al., 1999; Fischer et al., 2000). Next to analyses of the chemical
and isotopic signals locked in microfossils skeletons, quantitative analyses of changes in the taxonomic composition of
microfossil assemblages by means of ecological models is common in palaeoceanography since Imbrie & Kipp (1971). This
approach assumes that the composition of marine plankton and benthos communities reflects the environment in which they
45 lived and that this information is stored within the sediment by their fossils. The hypothesis that an assemblage of taxa can
be expressed as a function of (a) certain environmental variable(s) (ter Braak, 1987), allows for quantitative modelling
applying transfer functions and analogue methods (from now on called transfer functions). Multiple microfossils like
planktonic foraminifera (e.g. Kucera et al., 2005), diatoms (e.g. Sha et al., 2014) and dinoflagellate cysts (dinocysts) (e.g. de
Vernal et al., 2005) have been used for environmental reconstruction applying multiple transfer function methods.
50 However, the key assumption of this approach requires that the assemblage composition is significantly related to the given
environmental parameter to reconstruct both at present for the purpose of calibration and in the past for the purpose of
reconstruction. In the presence of multiple environmental parameters affecting assemblage composition, it is challenging to
disambiguate the effect of each parameter and determine which one(s) acted on the analysed fossil assemblages in the past.
There is evidence that the assemblages of zooplankton microfossils, such as planktonic foraminifera and radiolarians being
55 exclusively oceanic, are primarily controlled by temperature (Morey et al., 2005; Hernández-Almeida et al., 2017).
Phytoplanktonic microfossils assemblages however, like diatoms and dinocysts, seem to be affected by multiple environmental
factors (de Vernal et al., 2000, 2001; Dale et al., 2002; Holzwarth et al., 2007; Radi and de Vernal, 2008; Ribeiro and Amorim,
2008; Lopes et al., 2010; Hohmann et al., 2020). Apparently, phytoplankton communities have a complex relationship to the
environment and reflect independently the attribute of hydrography and nutrient availability, rendering the possibility of
60 multiple environmental factor reconstruction. It is tempting to explore whether such dependency on multiple factors can be
used to reconstruct changes in all the driving factors in the past.

About 20 % of dinoflagellate species produce organic-walled cysts within their life cycles (Wall and Dale, 1968; Dale, 1983;
Taylor and Pollinger, 1987; Head, 1996). As the walls of these cysts consist of a condensed predominantly aromatic
macromolecular structure (Kokinos et al., 1998), they are relatively good preserved in seafloor sediments (e.g. Zonneveld et
65 al., 2008), not being prone to dissolution after death, unlike mineralised fossils as calcareous (e.g. foraminifera and
nannoplankton) or siliceous (e.g. diatoms and radiolarians) microfossils (Koç et al., 1993; Matthiessen et al., 2001;
Seidenkrantz et al., 2007; Schröder-Adams and van Rooyen, 2011; Zamelczyk et al., 2012). However, during exposure on the



seafloor oxidation of the dinocyst may result in selective organic matter degradation which might affect the assemblage composition (Zonneveld et al., 2010). Nevertheless, if organic matter degradation is negligible, in settings with carbonate or opal dissolution, dinocyst-based transfer functions are often the best means to reconstruct past surface ocean properties.

Dinoflagellates form a major group of planktonic marine primary producers and include diverse autotrophic, mixotrophic, and heterotrophic forms that all thrive in the upper layers of the oceans (e.g. de Vernal and Marret, 2007). Dinocyst studies of marine surface sediment samples revealed that dinocysts are excellent tracers of hydrological and biological conditions (Mudie, 1992; Rochon and Vernal, 1994; Matthiessen, 1995; de Vernal et al., 1997, 2000, 2001, 2013; Radi et al., 2001; Radi and de Vernal, 2004, 2008; Rochon et al., 2008). While dinocyst assemblages can theoretically be applied to quantify multiple environmental drivers, identification of the primary driving factor(s) for the dinocyst assemblages compositional changes is challenging. Relationships between the assemblages and environmental parameters are complex, pointing to regionally different relationships between assemblages and environmental conditions. For example, whereas temperature and salinity gradients are determinants in the Atlantic-Arctic region, primary productivity seems to explain a large portion of taxonomic variability in the Pacific (Radi and de Vernal, 2008; Hohmann et al., 2020). Studies suggest that the number and type of primary factors driving dinocyst assemblages vary regionally (Zonneveld and Siccha, 2016; Hohmann et al., 2020). Additionally, the evaluation of the performance of transfer functions seems to be method-specific (Hohmann et al., 2020) and biased by spatial autocorrelation (Telford and Birks, 2005, 2009).

Hohmann et al. (2020) analysed the dimensionality of the dinocyst environmental response separately for assemblages from the Pacific and the Atlantic-Arctic regions, calibrated and evaluated multiple transfer-function methods for predicting environmental variables and estimated their performances in the light of spatial autocorrelation. This study identified different primary drivers for two areas affecting dinocyst assemblage composition, highlighting the merit of local calibrations and the necessity to carry out variable selections of main driving factors for each study area separately. Defining a local calibration dataset has the advantage of reducing the complexity of the assemblage to environment composition. However, this comes at the cost of reducing the pool of compositional variability, leading to the risk of biasing the results. For example, in Holocene cores off West Greenland, some of the best compositional analogues have been found in the Gulf of St. Lawrence (e.g. Allan et al., 2018).

However, because factor(s) driving microfossil assemblages differ between regions, it is possible that the same fossil assemblages may find equally good compositional analogues representing different combinations of environmental parameters. Hence, while local calibrations limit the range of compositional variability available to derive the transfer function, they are more likely to disambiguate the main driving variable in a certain region, which may render reconstructions in that region more robust assuming the driving factors remain the same.

By calibrating locally, we can exclude areas where dinocysts are susceptible to lateral transport during sinking and sedimentation processes. There is evidence that a dinocyst could be displaced up to thousands of kilometres from the location at the surface where it was produced (Nooteboom et al., 2019). Long-distance cyst transport by bottom waters and sediment



flows was also suggested based on sediment trap studies in the central and North Atlantic Oceans (Dale, 1992; Dale and Dale, 1992). This implies that in areas with strong ocean currents, the surface above the sedimentation area does not necessarily mirror the environmental conditions under which the plankton was produced, generating a nuisance in the calibration dataset.

The aim of this study is to investigate if a local dinocyst-based transfer function calibration on samples covering the Baffin Bay and surrounding regions allows a robust disambiguation of the factors that affected the assemblage variation in this region during the Holocene. Baffin Bay is a climate-sensitive region characterised by strong seasonal sea ice variability and meltwater discharge from the Greenland Ice Sheet (GIS). In view of the current rapid warming in the Arctic, it is relevant to understand how this marine basin reacted to climate changes during the Holocene. Indeed, to this end, many Holocene reconstructions based on fossil dinocyst assemblages were made and could serve as a basis for a comprehensive analysis of factors affecting the assemblage composition (e.g. Levac et al., 2001; Ouellet-Bernier et al., 2014; Allan et al., 2018; Caron et al., 2019).

We begin by carrying out an objective variable selection, guided by canonical ordination, and investigate the data structure of the resulting designed local transfer functions. We proceed by testing their ability to interpret assemblage changes recorded in Holocene sediments by their applications on four records covering a North-South transect throughout the Baffin Bay area. To this end, we used data from three existing records and added new data from a core located in Southern Melville Bay (see Fig. 1(a) and Table 1). We specifically focus on Holocene sections, assuming that the magnitude of environmental change in the Holocene was relatively small for the local calibration to be sufficient to capture the range of past environments recorded in the cores. To estimate the significance of the reconstructions we apply a test designed by Telford and Birks (2011), evaluating if reconstructions explain more of the variation in the fossil taxa data than random environmental variables assigned to the same fossil data. To assess the merit of a local versus a larger regional calibration, we compared local transfer function results to regional transfer functions based on a Northern Hemisphere calibration dataset.

125

130



135 **Table 1: List of cores used in this study.** Including core location and water depth (m), the modern sea surface conditions: sea surface temperature (SST) in summer, sea surface salinity (SSS) in summer, months per year of sea ice cover, and annual productivity of organic carbon for each location provided by the WOA and NSIDC.

Core ID	Core location	Latitude (° N)	Longitude (° W)	Water depth (m)	Modern sea surface conditions				Time interval covered (yrs BP)	References for dinocyst records
					SST summer (°C)	SSS summer (psu)	Sealce (month yr ⁻¹)	PPannual (mgC m ⁻² day ⁻¹)		
HU91-039-008P	Nares Strait	77.16	74.19	663	1.42	31.93	7.64	4635.00	1549-6756	Levac et al. 2001
GeoB19927-3	Southern Melville Bay	73.35	58.05	932	3.89	32.74	7.22	4179.00	0-7677	This paper and Saini et al. 2020
MSM343310	Disco Bugt	68.38	53.49	855	5.45	32.54	3.84	6374.00	135-3578	Allan et al. 2018
HU2008-029-004	Northwest Labrador Sea	61.46	58.03	2674	7.31	34.16	0.72	4497.00	0-9936	Gibb et al. 2015

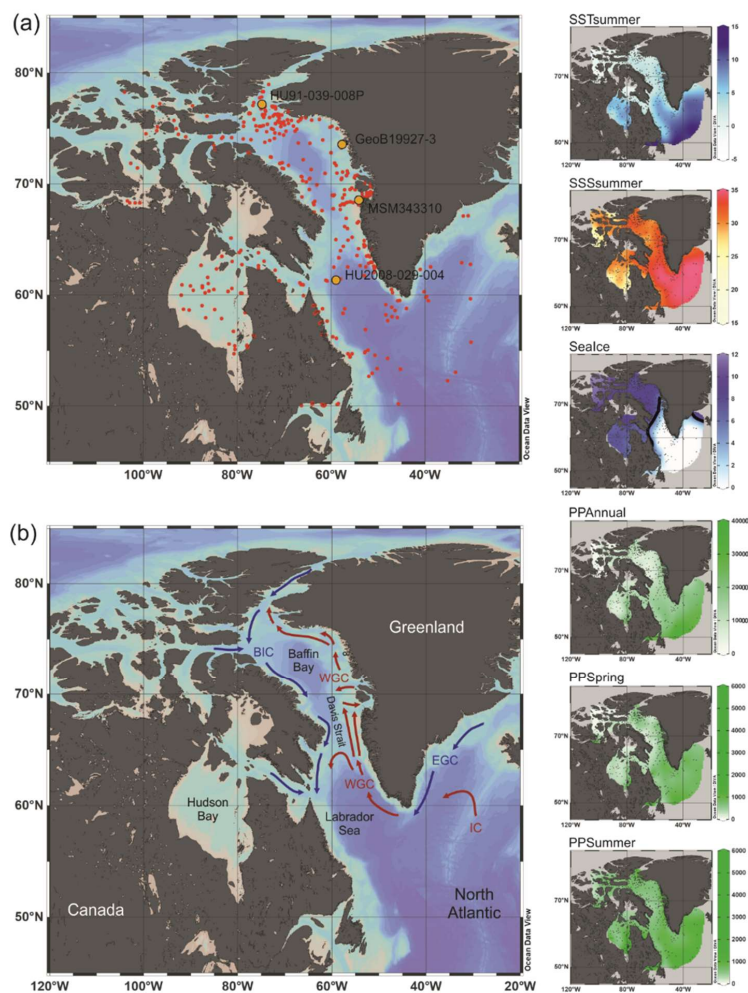


Figure 1: Map of the study area. (a) Location of surface sediment samples (red dots) from the calibration dataset and cores (orange dots; see Table 1) used in this study; (b) Schematic modern surface water circulation in the Baffin Bay area and around Greenland (BIC – Baffin Island Current, WGC – West Greenland Current, EGC – East Greenland Current, IC – Irminger Current). On the right, modern environmental parameter gradients gridded using DIVA gridding with Ocean Data View (Schlitzer 2018). Units are listed in Table 3. The six-month sea-ice edge in the sea-ice gradient map is indicated by the thick black line.



2 Material and methods

150 2.1 Data

The calibration dataset includes a local subset of the data from the Northern Hemisphere dataset (n=1968) in de Vernal et al. (2020). The local subset comprises census counts of recent organic-walled dinoflagellate cyst assemblages from core-top sediments at 421 sites from Baffin Bay with Kane Basin, Norwegian Bay, and Lancaster Sound (n=233), Davis Strait (n=103), Labrador Sea (n=30) and Hudson Bay with Hudson Strait and Foxe Basin (n=55) (Fig.1a). In samples containing low dinocyst concentrations, minimum counts of 60 specimens were accepted. The core-top samples were collected in the uppermost 1 cm of box or gravity cores and represent a few tens of years to centuries, depending upon sedimentation rates and mixing due to bioturbation (Radi and de Vernal, 2008). Palynological sample processing followed the procedures for palynological preparation described in de Vernal et al. (2010), which exclude the use of oxidation techniques to avoid selective degradation of more sensitive cyst taxa such as those produced by Protoperidinales (Marret, 1993). The Northern Hemisphere dataset from (de Vernal et al., 2020) served also as the regional reference dataset which we use to compare the results of the local dataset to. With exception of the samples from Price et al. (2016, 2018), which were added at a later stage, the Northern Hemisphere dataset and therefore all samples included in the local dataset have been tested negative for a significant selective organic matter degradation (Zonneveld et al., 1997) in Hohmann et al. (2020). The taxonomy used corresponds to that presented in Rochon et al. (1999) and updated in van Nieuwenhove et al. (2020). The taxonomic resolution of the local dataset was reduced to 33 dinocyst taxa after grouping following Hohmann et al. (2020) (Table 2, List of taxa). The original dinocyst dataset holding taxon percentages is archived at PANGAEA (de Vernal et al., 2019); the local data matrices with reduced taxonomy used in this analysis are available as supplementary material (S1).

We chose to carry out a canonical-ordination-based parameter selection (Lopes et al., 2010) to characterise the relationship between environmental variables and dinocyst assemblage composition. We defined a set of potential environmental controlling variables for dinocyst distributions in the Baffin Bay region: surface layer (here represented by conditions at 0 m depth) temperature and salinity in summer, sea ice cover and productivity in spring and summer as well as for the whole year. We did not consider temperature, salinity, and productivity parameters for the cold seasons since most of the area is covered by sea ice and there is hardly any productivity and hence no dinocyst production. Apart from environmental factors, some life-cycle factors (e.g., Fensome et al., 1993) such as water depth and distance from shore seem to affect dinocyst assemblages. But as they represent a separate independent dimension of variance (Hohmann et al., 2020), we do not include them in the local calibration dataset. The initial variable selection is listed in Table 3 and includes some of the variables considered in Hohmann et al. (2020) (c.f. for more detail). Their spatial distribution is shown in Fig. 1.

Table 2: List of dinocyst taxa in the local calibration dataset. Including abbreviations and highest relative abundances (minimum is always zero). Asterisks indicate heterotrophic taxa.

Taxa name	Abbreviation	Notes	Maximum %
-----------	--------------	-------	-----------



<i>Ataxiodinium choane</i>	Atax		1.2
<i>Bitectatodinium tepikiense</i>	Btep		3.3
<i>Impagidinium aculeatum</i>	Iacu		2.1
<i>Impagidinium pallidum</i>	Ipal		7.5
<i>Impagidinium paradoxum</i>	Ipar		8.8
<i>Impagidinium patulum</i>	Ipat		1.8
<i>Impagidinium sphaericum</i>	Isph		6.2
<i>Nematosphaeropsis labyrinthus</i>	Nlab		71.6
<i>Operculodinium centrocarpum</i>	Ocen	Group including: <i>Operculodinium centrocarpum</i> , <i>O. centrocarpum</i> — short processes, <i>O. centrocarpum</i> — Arctic morphotype	93.5
<i>Pyxidiniopsis reticulata</i>	Pret		1.5
<i>Spiniferites elongatus</i>	Selo		27.3
<i>Spiniferites ramosus</i>	Sram		14.6
<i>Spiniferites lazus</i>	Slaz		0.3
<i>Spiniferites mirabilis-hyperacanthus</i>	Smir		0.6
<i>Spiniferites</i> spp.	Sspp		4.4
Cyst of <i>Pentapharsodinium dalei</i>	Pdal		95.3
Cyst of <i>Scrippsiella trifida</i>	Stri		4.2
<i>Islandinium minutum</i> *	Imin	Group including: <i>Islandinium minutum</i> *, <i>Islandinium ? cesare</i> *, <i>Islandinium brevispinosum</i> *	96.8
<i>Echinidinium karaense</i> spp.*	Ekar		19.6
<i>Brigantedinium</i> spp.*	Bspp	Group including: <i>Brigantedinium</i> spp., <i>Brigantedinium cariacense</i> , <i>Brigantedinium simplex</i> , Cyst of <i>Protopteridinium americanum</i> *	99.0
<i>Dubridinium</i> spp.*	Dubr		3.4
<i>Protopteridinioid</i> cyst*	Peri		1.3
<i>Lejeunecysta</i> spp.*	Lspp		0.7
<i>Selenopemphix nephroides</i> *	Snep		2.2
<i>Xandarodinium xanthum</i> *	Xxan		0.9



<i>Selenopemphix quanta</i> *	Squa	Group including: <i>Selenopemphix quanta</i> *, Cyst of <i>Protoperidinium nudum</i> *	20.8
<i>Trinovantedinium applanatum</i> *	Tapp		5.2
<i>Votadinium calvum</i> *	Vcal		0.5
<i>Votadinium spinosum</i> *	Vspi		0.6
<i>Quinquecupis concreta</i> *	Qcon		0.7
Cyst of <i>Polykrikos kofoidii</i> *	Pkof		8.6
Cyst of <i>Polykrikos</i> sp. – Arctic*	Parc		23.1
<i>Echinidinium</i> spp.*	Esp		2.5

185 **Table 3: Environmental variables used in the canonical-ordination based parameter selection and their ranges within the local calibration dataset.**

Environmental variable	Minimum	Maximum	Range
SSTsummer [°C]	-0.81	13.24	14.05
SSSummer [psu]	17.51	34.98	17.47
Sealce [months yr ⁻¹]	0	12	12
PPAnnual [mgC m ⁻² day ⁻¹]	824	33047	32223
PPSpring [mgC m ⁻² day ⁻¹]	64	3626	3562
PPSummer [mgC m ⁻² day ⁻¹]	202	6021	5819

We used four sediment sequences to test the ability of the locally calibrated transfer functions to interpret assemblage changes during the Holocene. These sediment cores cover a North-South transect throughout the Baffin Bay region (Fig.1(a), Table 1) including intervals within the last 10 ka.

We analysed dinocyst assemblages in core GeoB19927-3 (73°35,26' N, 58°05,66' W), which was taken at 932 meters of water depth by gravity coring during cruise MSM44 in 2015 (Dorschel et al., 2015). This core is from southern Melville Bay, an area where the relatively warm high-salinity West Greenland Current (WGC) interacts with the cold polar water of the Baffin Current (BC) originating from the Arctic Ocean and meltwater from glaciers of the North-West Greenland region. It is located optimally and offers a high resolution and continuous sedimentation (Dorschel et al., 2016). A high-resolution radiocarbon-based chronology and organic biomarker proxies for sea ice and primary productivity have already been presented by Saini et

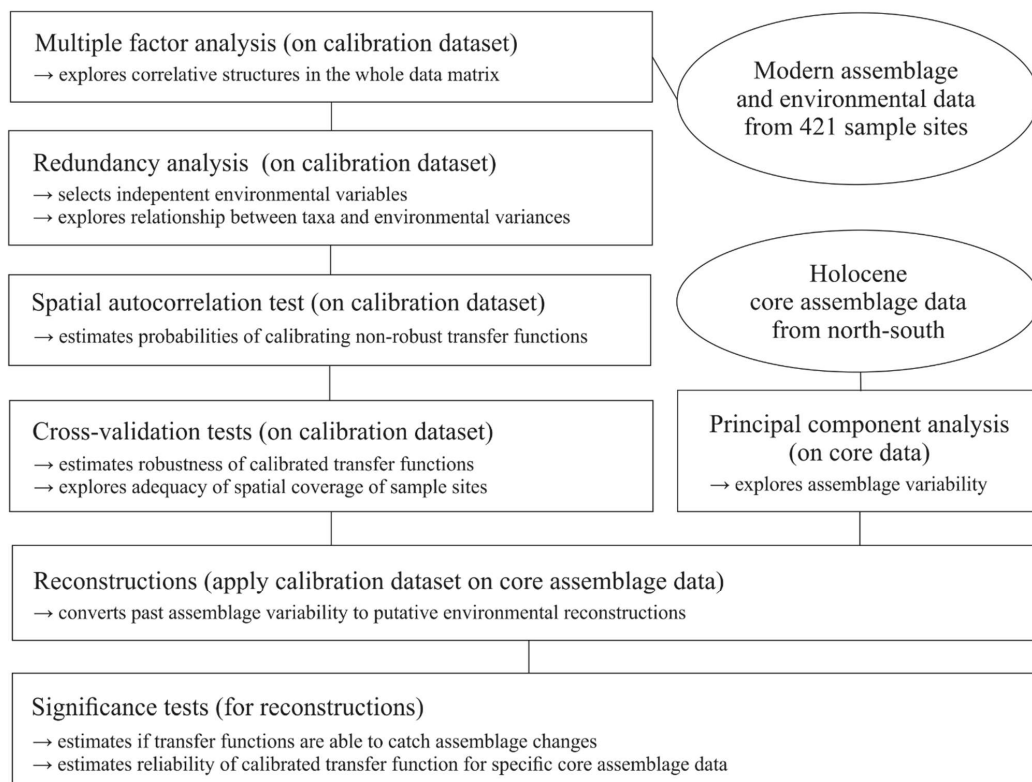


al. (2020). The core consists of 1147 cm of sediment. The working half of the core was sampled and divided into four sets of samples. One set was freeze-dried for dinocyst analysis. The other three sets were stored for other multi-proxy analyses and chronology (i.e., biomarker, foraminifera, and provenance studies). In reference to summer temperature anomalies during the Holocene for the Northern Hemisphere (Marcott et al., 2013; Kaufman et al., 2020), we expected a possible trend towards the last 2000 years and sampled at a higher resolution within the top 270 cm. We sub-sampled every centimetre within the top 25 cm, every 5 cm within the 25 cm to 280 cm interval, and every 10 cm within the 280 cm to 760 cm interval covering the last 7677 years, including 124 samples (see Table 1). Sample processing followed the procedure for palynological preparation described in de Vernal et al. (2010), which consists of repeated HCl and HF treatment. The taxonomy of dinocysts used here was based on Rochon et al. (1999) and de Vernal et al. (2020), considering all taxonomic categories that were resolved in the calibration dataset. To obtain statistically reliable assemblage counts, at least 300 dinocyst specimens were counted per sample when possible. For samples with low dinocyst abundance as many specimens as possible were enumerated. For the sample with the lowest dinocyst abundance, we counted 89 specimens. The raw assemblage dataset for GeoB19927-3 will be available on time via the PANGAEA database.

In addition, we re-evaluated three existing sediment records that have already been studied in detail and have been analysed for their palynological content and dinocyst assemblages. HU91-039-008P (Levac et al., 2001) was sampled every 20 cm from the top to 820 cm which corresponds to 1549-6756 years BP and includes 41 samples. MSM343310 (Allan et al., 2018) includes 194 samples taken around every 8 cm from top to 925 cm (135-3578 years BP), while HU2008-029-004 (Gibb et al., 2015) includes 30 samples from every 4 cm from top to 116,5 cm (0- 9936 years BP) (see Table 1).

2.2 Data analysis

To explore the local relationship between dinocyst assemblages and environmental variables, we followed the procedure schematically illustrated in Fig. 2 and used statistical ordination (McGarigal et al., 2000). We performed detrended correspondence analysis (DCA) (Birks, 1995) to evaluate the gradient length, expressed as standard deviation (SD) units in the first DCA axis to decide whether to apply linear ($SD < 3$) or unimodal ordination ($SD > 4$; $SD > 3$ to < 4 both methods possible but unimodal ordination is advised) (Lepš and Šmilauer, 2003). For DCA and further analyses, we used the vegan package (Oksanen et al., 2019) in R (R Core Team, 2017). The dataset was found to have an SD of 3.0 (S2 - supplementary data) using log-transformed ($\log(x+1)$) dinocyst assemblage per mil data. As the SD of our dataset is biased towards the linear threshold, we proceeded with linear techniques.



230 **Figure 2: Flowchart describing the approach and sequence of analyses in this study.**

In the first step, we used multiple factor analysis (MFA), an integration of multivariate matrices, to simultaneously couple several groups of variables that are defined on the same objects (Escofier and Pagès, 1984, 1990, 1994) with the aim of identifying a common or representative structure in the whole data matrix. MFA proposes a symmetrical, exploratory point of view, where correlative structures are exposed without any reference to the directionality of possible causal relationships. It is a simple co-inertia analysis that finds common structures in all or some of the data groups (Dray et al., 2003) and has previously been used in ecological studies (e.g. Beamud et al., 2010; Carlson et al., 2010; Lamentowicz et al., 2010). As all variables in this study are numerical, the MFA can be seen as a principal component analysis (PCA), wherein the first step each data group is analysed, weighted, and normalised by dividing all its elements by the first eigenvalue obtained from the PCA. In the second step, the normalised data groups are merged into a common matrix and a global PCA is performed.



We defined three data groups: One community dataset holding **dinocyst taxa ratios (33 taxa)** and two groups holding abiotic variables describing productivity (PPAnnual, PPSpring, PPSummer) and physical water properties (SSTsummer, SSSsummer, SeaIce). All three groups hold exclusively quantitative variables. **Hellinger-transformation (Rao, 1995)** was applied to the **dinocyst ratios** in the community data set. This transformation, as proposed by Legendre & Gallagher (2001) for a PCA with
245 community data containing many double-zero abundances, allows using PCA without considering the common absence of species as a resemblance between communities and preserves the Euclidean distance of a PCA when unimodal data is used, which might be possible as the SD of 3.0 might imply unimodal data. After Hellinger-transformation, the data from all three groups **was** standardised by scaling variables to a standard deviation of 1 and a mean of 0. The affinity between the group derived from the MFA is measured by their RV coefficient, ranging from 0 to 1 (Robert and Escoufier, 1976), which is tested
250 by a Pearson type III approximation (Josse et al., 2008). MFA computations were performed with the FactoMineR (Lê et al., 2008) and factoextra (Kassambara and Mundt, 2017) R packages.

We continued selecting the main drivers affecting compositional changes in the dinocyst assemblages. We applied Redundancy Analysis (RDA), a constrained ordination (McGarigal et al., 2000) for linear data, to quantify the strength of the relationship between species variances and the tested forcing parameters. Again, we applied Hellinger-transformation (Rao, 1995) to the
255 **taxa ratios** to ensure the preservation of Euclidean distance in the linear ordination as our species data SD did not indicate strongly linear data. Hellinger-transformation also gives less weight to species with low counts and many zeros, focussing more on the composition of common species, as we assume that local datasets unlike global ones do not include indicators or inter-regional endemic species. Environmental data were standardised as described above to ensure the compatibility of variables for comparisons.

RDA was performed after ter Braak (1986) using the **software** R (R Core Team, 2017). For the variable selection, we followed the procedure described in Hohmann et al. (2020), which includes a variable selection considering Variance Inflation Factors (VIFs) ≤ 2 with the objective to extricate independent variables that show no collinearity between each other and explaining a significant amount of the variance in the species data. Following this procedure, we obtained a set of three independent forcing variables, meaning that each of these three parameters explains a separate dimension of variance in the taxa data (for more
260 explanation see S3 – supplementary data). These three independent variables, that revealed to be summer sea-surface temperature (SSTsummer), summer sea-surface salinity (SSSsummer), and spring productivity (PPSpring) (see section 3.2), were used for a final RDA and further analyses.

We determined the extent and type of autocorrelation in the independent data set, as an accurate evaluation of transfer function performances is only possible in case of spatial independence between sample sites in the data set (Telford and Birks, 2009).
270 In the case of spatial autocorrelation, the transfer function performances can be overestimated, which could result in inappropriate choices of transfer function models and parameters, possibly including environmental variables with no ecological relevance as “reconstructable”. Autocorrelation could occur due to spatial interdependence of proxy variables, which would render the main requirement of spatial independence for adequate transfer functions violated. It could also be due to an environmental similarity of nearby sample sites. A spatial autocorrelation due to environmentally similar sites, as



275 found in data sets from the North Pacific as well as the North Atlantic and Arctic (Hohmann et al., 2020), may meet the
requirement of transfer functions. For autocorrelation tests and further analyses, we additionally used R packages fields
(Nychka et al., 2017), palaeoSig (Telford, 2015), and rioja (Juggins, 2017) implementing the routines developed in Telford
and Birks (2009).

For the transfer functions remaining in the independent calibration dataset, we did calibration and cross-validation based on
280 the leave-one-out (LOO) (cf. Efron and Gong, 1983) and h-block technique (Burman et al., 1994; Telford and Birks, 2005,
2009) for three distinctly different transfer function approaches: the Maximum Likelihood (ML), the Weighted Averaging
Partial Least Square (WA-PLS) and the Modern Analogue Technique (MAT). For calibration and cross-validation tests we
additionally used R packages bioindic (Guiot and Gally, 2014), gstat (Pebesma, 2004), and sp (Pebesma and Bivand, 2005)
and followed the R code developed by Trachsel and Telford (2016) for h-block cross-validation and the estimation of h (for
285 more details see Hohmann et al., 2020).

We reconstructed the three independent variables (SSTsummer, SSSsummer, and PPSpring) within four sediment sequences
collected along a north-south transect through the Baffin Bay area. To determine assemblage zones in each core we performed
principal component analysis (PCA) on percentages of downcore dinocyst assemblages.

We tested the ability of the calibrated transfer functions to interpret the assemblage changes recorded in the sediments by
290 applying the Telford and Birks method (2011). To estimate the significance of the reconstructions, this method evaluates if
reconstructions explain more of the variance in the fossil data than most reconstructions derived from transfer functions trained
on random environmental data. It also determines the best reconstruction when reconstructing several environmental variables
and if there is sufficient information in the proxy data to support multiple independent reconstructions. We use redundancy
analysis (RDA) to estimate the proportion of variance in the fossil data explained by a single reconstruction. Then, using the
295 same taxa data from the calibration dataset, reconstructions are inferred from transfer functions trained on random
environmental variables drawn from a uniform distribution. The proportion of the variance explained by these random
reconstructions is then estimated. If the tested variable explains more of the taxa variance than 95 % of the random
reconstructions, the reconstruction is deemed statistically significant (cf. Telford and Birks, 2011). Reconstructions that fail
this test should be interpreted with caution.

300 Reconstructions and significance tests within the four cores were performed by applying the calibrated local dataset (n=421)
and the regional Northern Hemisphere dataset (n=1968), aiming to assess the advantages and disadvantages of using the local
dataset.

3 Results

305 3.1 Multiple factor analysis

The MFA provides an informative view of the two main gradients and the relationship among the three defined groups of
variables. The first two axes represent about 31 % of the total variance. Figure 3 illustrates the correlation between the three
defined groups and the first two dimensions of the MFA. Temperature variables (SSTsummer and SeaIce) from the group of



physical water properties contribute the most to the first dimension followed by productivity and some dinocyst species. Within
 310 the second dimension, salinity contributes the most, followed by productivity and some dinocyst species. The correlation circle
 (Fig. 3a) shows the relationship between single variables, their quality of representation within the first two dimensions, as
 well as the correlation between single variables and dimensions.

The first dimension mainly represents the negatively correlated physical water properties, SSTsummer and SeaIce, while the
 second dimension is mostly represented by SSSsummer. Hence, we recognise the main gradient to be described by a transition
 315 from warmer and lesser sea-ice conditions to colder and exceeding sea-ice conditions with *Islandinium minutum* and the Cyst
 of *Polykrikos* sp. – Arctic characterising the colder end and *Bitectatodinium tepikiense* and *Selenopemphix quanta* the warmer
 end. The patterns of species vs environment relationships are further illustrated by the RV coefficients (Table 4).

Table 4: RV coefficients. The coefficients appear in the lower-left triangle below the diagonal, while the upper-right triangle contains the
 320 p values among the four groups of variables used in the MFA.

	Dinocyst Community	Physical Water Properties	Productivity
Dinocyst Community	1.000	< 0.01	< 0.01
Physical Water Properties	0.338	1.000	< 0.01
Productivity	0.117	0.327	1.000

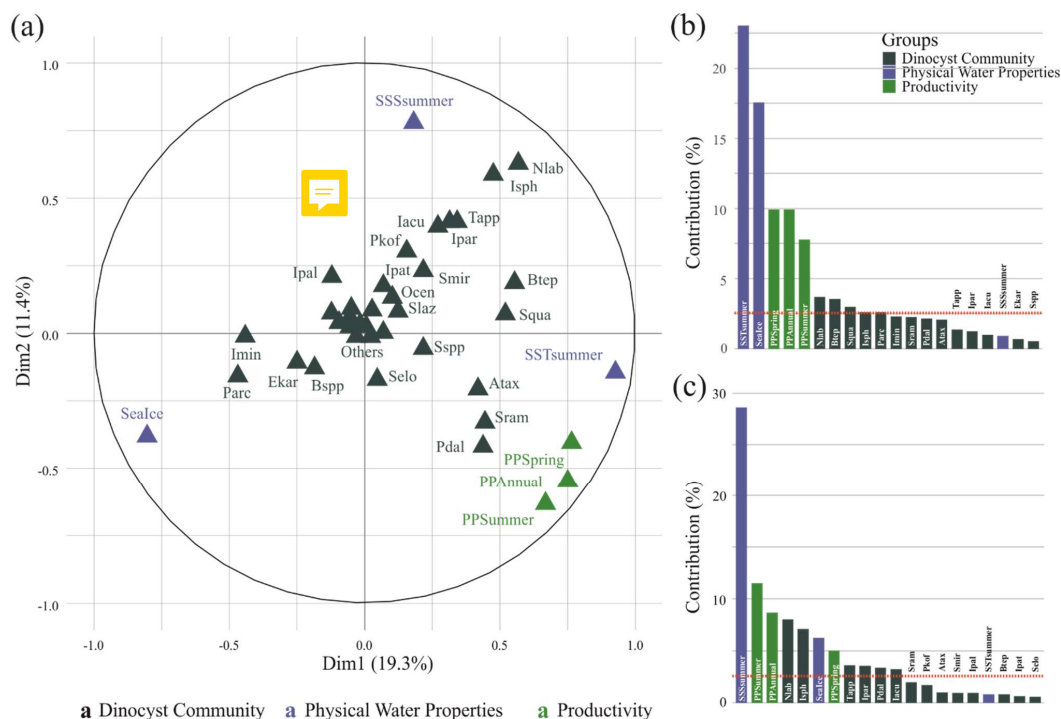


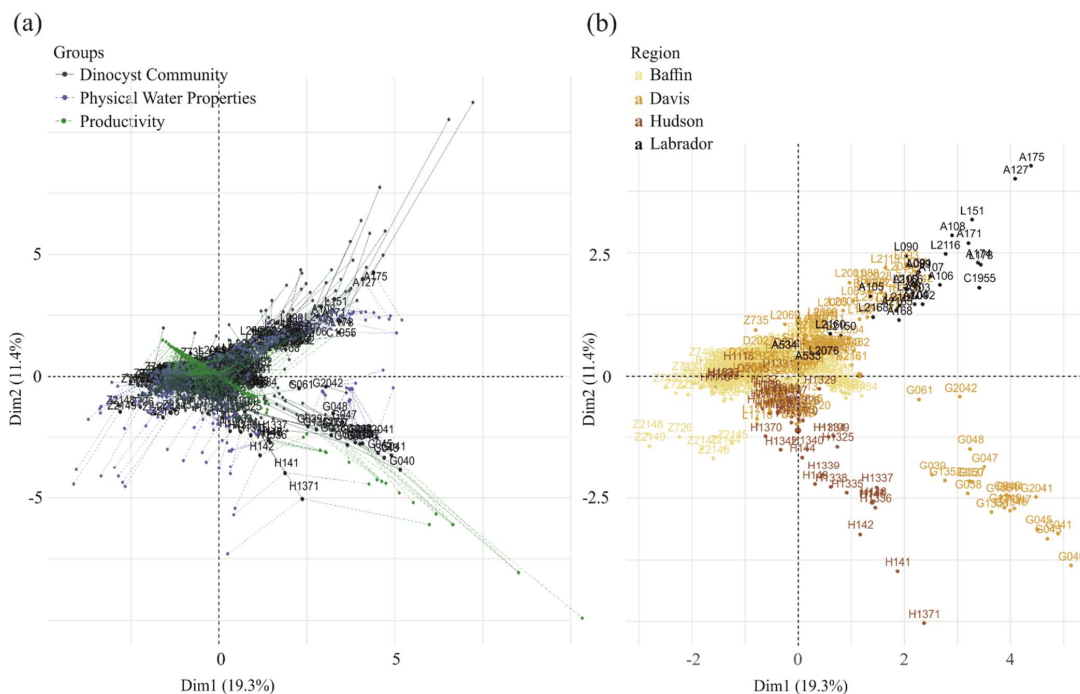
Figure 3: Contribution of the groups to the first two dimensions of the global PCA. (a) Correlation circle of variables after MFA. The distance between the variable points and their origins represents the weight of the variable within the first two dimensions. The variables the most correlated with a dimension lie close to the dimension's axis. Positively correlated variables are grouped together, while negatively correlated ones lie on opposite sides. (b and c) Contribution of the variables to the first and second dimensions, respectively.

Figure 4b illustrates sample site scores by their regional origins from the global PCA. Sample sites from the Labrador Sea and some sites from the Davis Strait mainly describe the first dimension. As emerged earlier, the first axis represents primarily a temperature gradient, pointing to a higher influence of temperature-related variables within the samples located along the first axis. The second dimension, thus salinity, is essentially associated with sample sites in Hudson Bay. Samples from Baffin Bay do not contribute much to the variance in the data matrix.

Figure 4a represents each sample site score with respect to the three groups. Larger black dots represent the site scores for the pooled MFA, while coloured dots connected with the black dots by coloured lines represent the separate PCA scores for each group. The highest contribution to productivity variances comes from sample sites in the Davis Strait, while the variance in



dinocyst communities can be attributed mainly to the Labrador Sea. Sample sites from the Labrador Sea, Hudson Bay, and some from Baffin Bay contribute to the variance in physical water property variables.



340

Figure 4: Sample sites within the first two dimensions of the MFA. (a) Sample site scores according to the pooled MFA with 421 data points (large black dots) and single PCAs depicting how much sample sites contribute to the variance in the data matrix in respect to the three groups. (b) Sample site scores relative to the first two dimensions of the global PCA. Sites with similar profiles are close to each other on the factor map.

345

3.2 Redundancy analysis

The first step of the variable selection is based on RDA carried out for single variables. It revealed that, when considered individually, each of the six environmental variables appeared to explain a significant ($p \leq .01$) amount of variation in the assemblage composition in the dataset (Table 5). Together, they explain 32 % of the total inertia in the taxa dataset. We then evaluated the independence of the tested environmental variables through a selection, excluding variables with VIF > 2. This successive forward selection uncovered three separate dimensions in the taxa variance driven by SSTsummer, SSSsummer

350



and PPSpring respectively. The remaining variables were excluded from further analyses due to their collinearity with SSTsummer, SSSsummer, or PPSpring.

355

Table 5: Explained inertia (as a single variable) and variance inflation factors of the tested environmental variables in the RDA model. VIF(a) when all variables are considered; VIF(b) after manual forward selection for variables without dependence.

Environmental variable	% inertia explained	VIF (a)	VIF (b)
	SSTsummer	12.4	3.9
SSSsummer	6.9	2.0	1.0
Sealce	9.7	2.9	
PPAnnual	4.2	394.7	
PPSpring	2.5	72.7	1.8
PPSummer	4.6	137.5	

360 When only the independent environmental variables are used, the constrained part of the RDA explains about 24 % of the taxa variance (Table 6) with environmental variables having significant correlations with RDA-axes (Table 7). The first axis explains 66 % of the constrained variance and is positively correlated with SSTsummer, while axes 2 and 3 explain 27 % and 7 % are positively correlated with SSSsummer and PPSpring, respectively (Fig. 5, Table 6). Regarding species-environment relationships, we find that the variance of *I. minutum* is strongly related to changes in SSTsummer, while the abundance of *N. labyrinthus* is related to SSSsummer. The cyst of *P. dalei* shows correlations with SSTsummer and PPSpring. Phototrophic cysts are generally associated with higher summer temperatures and heterotrophic cysts with lower temperatures (Figs. 5a-c). Sample-environment relationships (Figs. 5d-e) reveal that all samples contribute to the variance in SSTsummer. The variance for PPSpring is high for samples from Labrador Sea, Baffin Bay and Hudson Bay, while SSSsummer variance is highest in samples from Davis Strait and Hudson Bay.

370

375



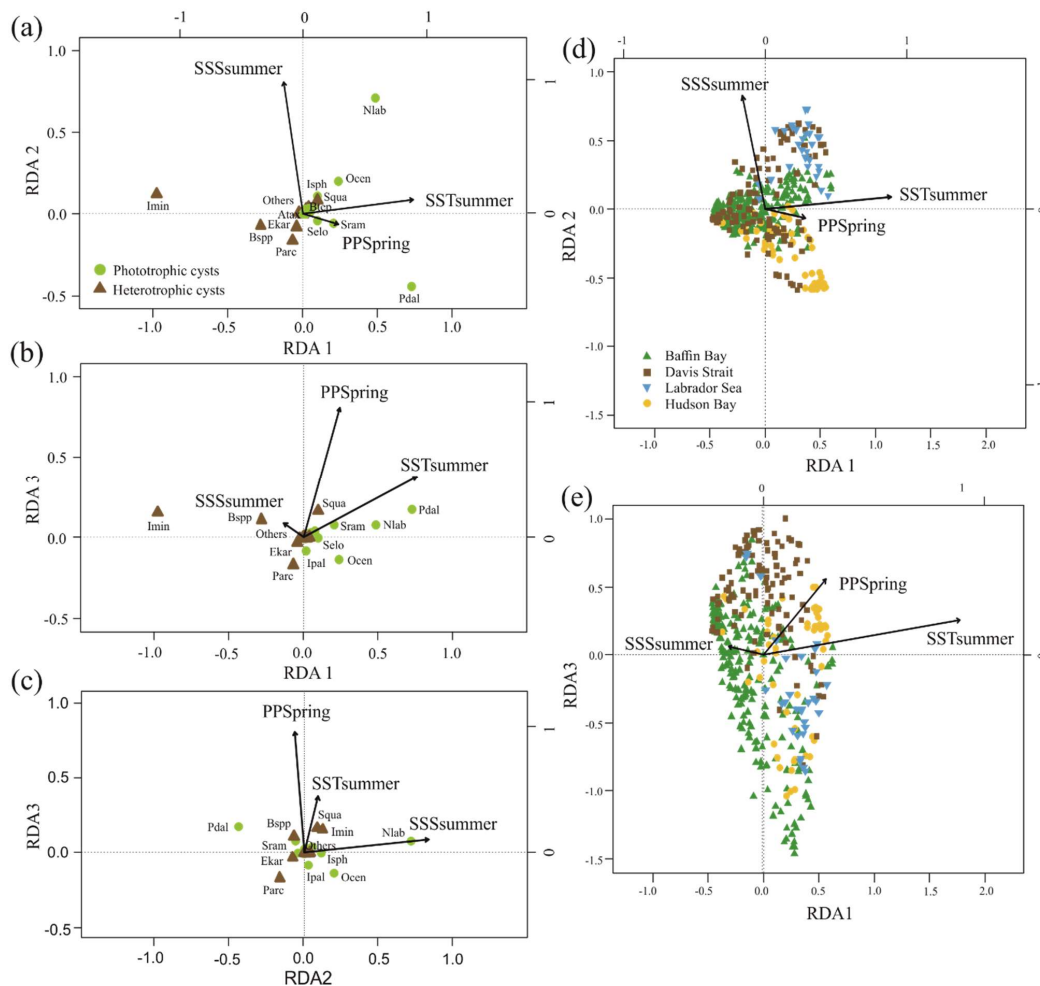
Table 6: RDA results and results of permutation tests for the significance of RDA-axes after manual forward selection ($p \leq .01$).

	RDA-axis 1	RDA-axis 2	RDA-axis 3	Total inertia	Proportion of total variance explained
Eigenvalues	0.057	0.024	0.005	0.365	
Constrained proportion explained	0.660	0.284	0.056		0.236
Constrained cumulative proportion	0.660	0.944	1.000		
F-value	85.2	36.6	7.3		

380

Table 7: Intrasect correlation coefficients (r^2) between independent variables and RDA-axes and between the variables themselves.

	RDA-axis 1	RDA-axis 2	RDA-axis 3	SSTsummer	SSSummer	PPSpring
SSTsummer	0.79	0.01	0.20	1	0.01	0.45
SSSummer	0.02	0.96	0.01		1	0.01
PPSpring	0.08	0.01	0.91			1



385

Figure 5: RDA scores. (a, b and c): RDA ordination diagrams of dinocyst taxa (see Table 1 for abbreviations) vs environmental variables (arrows) showing the correlation with the axes (direction of arrows) and the strength of the dinocyst vs environmental variable relationship (length of arrows). Species in the centre region are without abbreviations. (d and e): Sample ordination for RDA constrained by independent environmental variables for axes 1, 2 and 3.

390



3.3 Spatial autocorrelation

We tested spatial and environmental autocorrelation, considering only the independent variables and following the procedure described by Telford and Birks (2009). Inevitably, the performance (r^2) deteriorates with increasing fraction of sites deleted
395 (S4 - supplementary data). We find that the deterioration of performance is much worse with neighbourhood deletion than with random deletion, indicating the presence of spatial autocorrelation. When deleting environmentally similar sites, we find a pattern of performance loss that is slightly worse for neighbourhood deletion than for environmental deletion. Hence, removing geographically close sites causes a higher decline in performance than when the same fraction of environmentally similar sites is removed, indicating spatial autocorrelation over environmental autocorrelation. Variable performances drop
400 below 0.55 when samples within a 200 km radius are deleted, implying that calibrated transfer functions need to be interpreted with caution.

3.4 Cross-validation

For transfer function development, LOO-cross-validation results indicate the best performances for MAT, with WA-PLS
405 RMSEP values on average around 40 % higher and ML RMSEP values on average by around 100 % higher, depending upon the variable (Table 8). The differences in LOO-RMSEPs between the calibration and the verification subsets for MAT show differences of 25 % for SSSsummer and 8% for PPSpring, indicating an inadequate spatial coverage for some areas within the regional subset for these parameters. For SSTsummer reconstructions the spatial coverage in the dataset seems to be sufficient. All three environmental parameters show similar performances within each reconstruction method. The h-block cross-
410 validation shows MAT RMSEP increasing by 60 %, 60 % and 95 % for SSTsummer, SSSsummer and PPSpring, respectively. RMSEPs of WA-PLS and ML remain largely unaffected by site deletion within the applied radius h for SSTsummer (1 %) and SSSsummer (7 %) (Table 8). For PPSpring RMSEPs increase by about 25 %.

An inspection of the distribution of residuals from cross-validation tests of the variables along their environmental gradient reveals uneven residual distributions for all independent variables. (S6 - supplementary material). For all transfer function
415 methods, the spatial structure of the residuals is complex and large residual values emerge regionally. For ML large over- and underestimations suggest that the method is inaccurate for reconstructions. For MAT and WA-PLS, we observe a systematic underestimation in the Labrador Sea, especially for SSTsummer and PPSpring and an overestimation in parts of Baffin Bay and Hudson Bay with especially large overestimations for PPSpring in Hudson Bay. However, residuals for SSSsummer reconstructions regarding MAT and WA-PLS are quite small, suggesting solid transfer functions.

420



425 **Table 8: Cross-validation performances.** Performance for $n = 421$ applying LOO-cross-validation and h-block cross-validation for MAT
(c - calibration dataset, v - verification dataset) with the number of analogues used (#ana.), for WA-PLS with the number of components
used (#comp.) and for ML. The number of analogues and components that will perform best during reconstructions (#ana. and #comp.) have
been determined calculating the RMSE of prediction as a function of the number of analogues used and a randomisation t-test for testing the
significance of cross-validated components used after van der Voet (1994), respectively. h-values have been estimated by fitting a spherical
430 variogram to detrended residuals of a WA model (S5 - supplementary material) following Telford and Birks (2009) as well as Trachsel and
Telford (2016).

Cross-validation	LOO													
Method	MAT					WA-PLS					ML			
	RMSEP _c	r ² _c	RMSEP _v	r ² _v	#ana.	RMSE	r ²	RMSEP	r ²	#comp	RMSE	r ²	RMSEP	r ²
SSTsummer	1.38	0.76	1.35	0.80	5	1.90	0.58	2.03	0.52	4	2.73	0.41	2.75	0.40
SSSummer	1.35	0.68	1.01	0.78	5	1.55	0.56	1.60	0.53	2	2.34	0.49	2.37	0.47
PPSpring	324.16	0.61	298.14	0.75	7	446.20	0.30	466.17	0.24	3	748.44	0.04	750.99	0.04
Cross-validation	h-block										h [km]	Variogram model		
Method	MAT			WA-PLS			ML							
	RMSEP	r ²	#ana.	RMSEP	r ²	#comp.	RMSEP	r ²						
SSTsummer	2.25	0.42	5	1.93	0.59	4	2.74	0.43	256	Spherical				
SSSummer	2.14	0.22	5	1.68	0.64	4	2.48	0.57	623	Spherical				
PPSpring	636.67	0.01	7	536.96	0.36	5	958.37	0.02	745	Spherical				

435

3.5 Transfer function significances in sediment core reconstructions

Having established the transfer functions, we applied them to the selected four sediment cores covering the N-S transect. First, for each record, we identified the interval characterised by the largest changes in assemblage composition, which we assumed to be related to the most important environmental change. PC analysis of downcore dinocyst assemblages revealed one to two
440 assemblage changes within each of the four cores (Fig. 6). The first component (PC1) of the PCA identified three assemblage



zones in the northernmost record HU91-039-008P, which account for 74.5 % of the total variance, while PC2 accounted for 17.0 %. In Southern Melville Bay (GeoB19927-3) and Disko Bugt (MSM343310) PC1 identified two assemblage zones accounting for 76.6 % and 77.7 % of the total variance, while PC2 identified at least three assemblage zones accounting for 17.0 % and 18.3 % respectively. Within the most southern record from the Labrador Sea (HU2008-029-004) PC1 revealed
445 four zones (69.3 %) and PC2 three zones (21.3 %).

The reconstructions based on the local calibration dataset for the northern core HU91-039-008P (Fig. 6a) show modest changes but SSTsummer resonates with the facies shifts. In core GeoB19927-3 (Fig. 6b), assemblage zone shifts correspond to variations in SSSsummer and PPSpring reconstructions based on ML and WA-PLS. In core MSM343310 (Fig. 6c), the facies shift is caught in SSSsummer and SSTsummer reconstructions based on ML and WA-PLS. In core HU2008-029-004 (Fig.
450 6d), we identify shifts based on WA-PLS and ML reconstructions. Cross-correlations between PCA-axis 1 and reconstructed SSTsummer, SSSsummer and PPSpring point to high correlation coefficients ($r^2 \geq 0.70$) applying ML and WA-PLS followed by MAT with lower correlation coefficients (S7 - supplementary material).

The different degree of correspondence between the environmental reconstructions inferred by the transfer functions and the principal community change trends in the dinocyst records is echoed in the significance tests made after the approach of Telford and Birks (2011) for downcore reconstructions. Here a significant reconstruction should explain more of the variance in the
455 fossil dinocyst assemblage than a random transfer function calibrated using the same assemblages but random environmental data. These tests reveal that different transfer function methods and environmental variables produce significant reconstructions for each core. Significance test results of transfer function applications with the local dataset and the regional Northern Hemisphere dataset reveal the same pattern (Table 9).

460 When the Northern Hemisphere dataset (n=1968) is used for reconstructions of the four downcore assemblages (Fig. 6), we find that 17 % of all the tested transfer functions produce significant estimates (SSSsummer – 25 %, SSTsummer – 17 %, PPSpring – 8 %) (Fig. 7, Table 9).

However, when applying the local calibration dataset (n=421), most transfer functions produce significant reconstructions for SSSsummer (75 %) and SSTsummer (50 %), and some for PPSpring (8 %) (Fig. 7, Table 9). For the northern core HU91-039-
465 008P, summer salinity estimates are significant with all three transfer function methods (Fig. 7a). In the Southern Melville Bay core GeoB19927-3, the WA-PLS transfer function has been tested as significant for PPSpring, as well as SSSsummer and SSTsummer (Fig. 7b). For records in Disko Bugt (MSM343310), both MAT and WA-PLAS produce significant estimates for SSSsummer, while WA-PLS shows additional significance for SSTsummer (Fig. 7c). Further south, the record from Labrador Sea (HU2008-029-004) yields significant estimates for SSSsummer and SSTsummer based on MAT and ML (Fig. 7d).

470

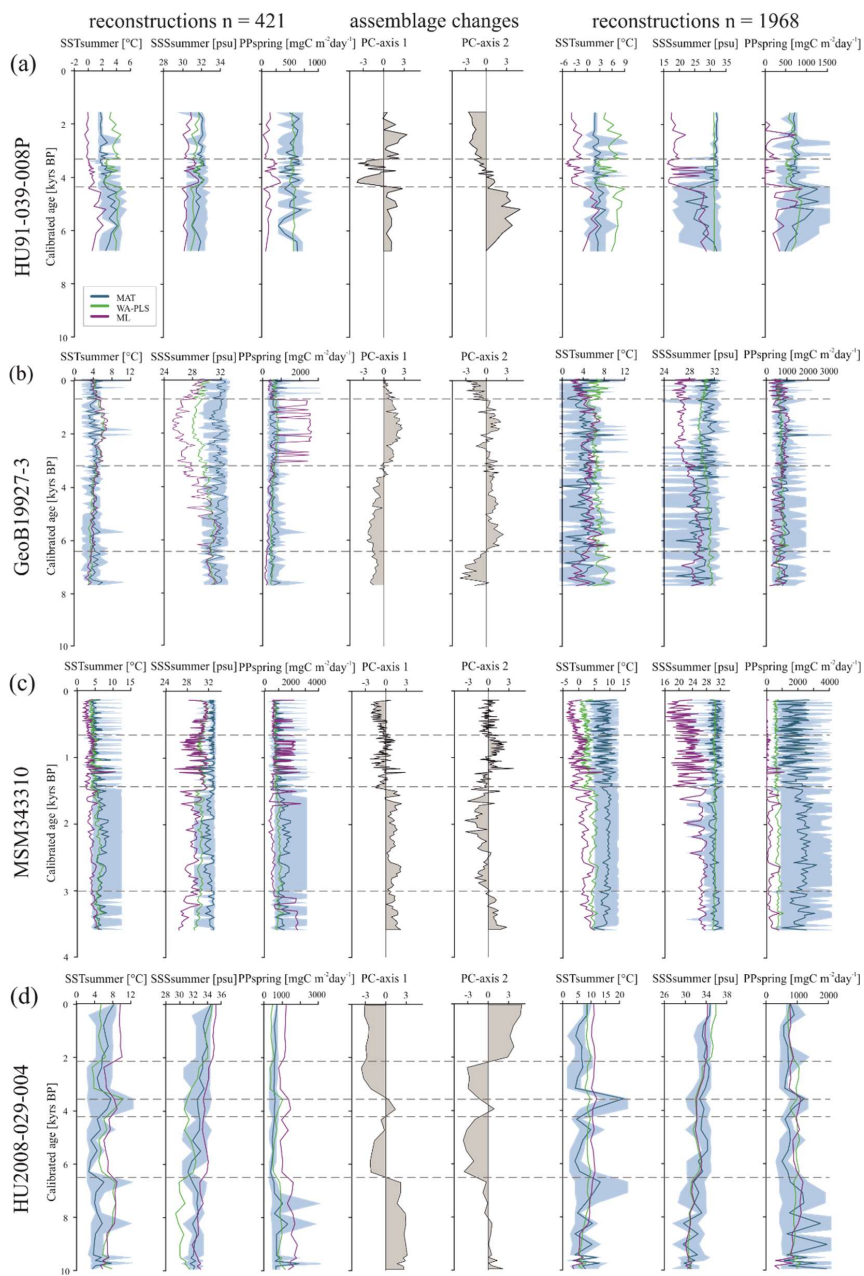




Figure 6: Downcore reconstructions based on the local dataset (n = 421) and the Northern Hemisphere dataset (n = 1968) using three transfer function techniques. MAT, WA-PLS and ML are represented by blue, green and purple curves respectively. The lighter blue curves correspond to maximum and minimum possible values calculated from a set of five modern analogues. The ecostratigraphic zones are determined from PC analyses. (a) HU91-039-008P, (b) GeoB19927-3, (c) MSM343310 and (d) HU2008-029-004.

Table 9: Significances for downcore reconstructions after the approach of Telford and Birks (2011) using the local dataset (n = 421) and the regional Northern Hemisphere dataset (n = 1968). Significant reconstructions are marked by a green check mark, and the not significant ones by a red cross.

Transfer function significances	function	n = 421			n = 1968		
		SSTsummer	SSSsummer	PPspring	SSTsummer	SSSsummer	PPspring
HU91-039-008P	MAT	✓	✓	×	×	✓	✓
	WA-PLS	✓	✓	×	×	×	×
	ML	×	✓	×	×	×	×
GeoB19927-3	MAT	×	×	×	×	×	×
	WA-PLS	✓	✓	✓	×	✓	×
	ML	×	✓	×	×	×	×
MSM343310	MAT	×	✓	×	×	✓	×
	WA-PLS	✓	✓	×	×	×	×
	ML	×	×	×	✓	×	×
HU2008-029	MAT	✓	✓	×	✓	×	×
	WA-PLS	×	×	×	×	×	×
	ML	✓	✓	×	×	×	×



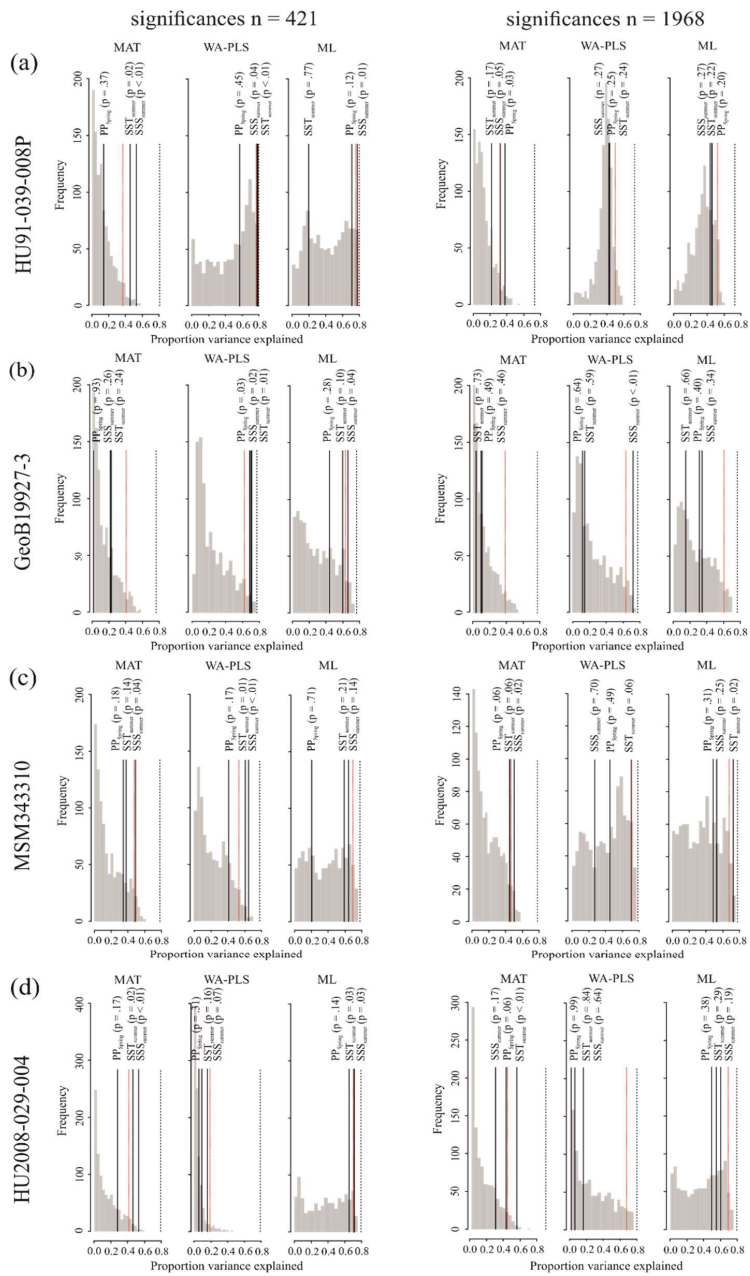




Figure 7: Results of the significance tests for downcore reconstructions. (a) HU91-039-008P, (b) GeoB19927-3, (c) MSM343310 and
485 (d) HU2008-029-004. For all significance tests, 999 random environmental variables were generated to produce the null distribution (grey
bars). Black lines mark the variances explained by observed variables. Red dotted lines mark the 95th percentile of the random distribution
($p \leq .05$) above which reconstructions are deemed as significant. The proportion of the variance explained by the first axis of a principal
component analysis (PCA) is also recorded (black dotted line), as this represents the maximum proportion of the variance in the fossil data
that a reconstruction could possibly explain. For significance test analysis we applied the number of analogues (MAT) and components
490 (WA-PLS) resulting in highest significances respecting all three variables.

4 Discussion

4.1 Methodology

The ecological models and transfer functions derived in this study rely on a few assumptions. Foremost is that the composition
495 of dinocyst assemblages was primarily affected by the selected environmental parameters and that the set of parameters is
comprehensive and includes all the relevant parameters. However, it is possible that a sedimentary assemblage reflects other
processes than the considered parameters. For example, non-oceanographic factors such as those related to the dinoflagellate
life cycle (Bravo and Figueroa, 2014) or post-depositional organic matter degradation (Zonneveld et al., 2019) could affect the
dinocyst assemblage composition in the calibration dataset. . The production of cysts is a part of the dinoflagellate's sexual
500 reproduction. It protects the diploid cell, which may be dormant for a variable length of time. After dormancy the cell emerges
from the cyst and re-establishes its metabolic activities within the pelagic ecosystem (Taylor and Pollinger, 1987). During
encystment many cysts settle on the seafloor, requiring areas where the seafloor is not too deep to ensure the possibility of
excystment and ascendance of the cells into surface waters. Hohmann et al. (2020) showed that water depth and distance from
shore explain a significant amount of compositional variance in dinocyst assemblages ($p < .01$). However, these variables were
505 shown to describe a separate dimension of variability, orthogonal to the tested oceanographic and primary productivity factors.
Also, when applied to a sedimentary record, factors such as the distance from shore and water depth should be mostly constant
for the downcore record. The effect of organic matter degradation on the dinocyst assemblage composition can be detected
independently of the ecological model because the ratio between cysts of autotrophic and heterotrophic taxa should
systematically decrease with an increase in selective organic matter degradation, caused by their different wall polymer
510 composition (Zonneveld et al., 1997). In the Northern Hemisphere calibration dataset, there is no evidence of a pervasive effect
of degradation. Neither in the Northern Hemisphere (Hohmann et al., 2020), nor in the Baffin Bay local dataset (this study) a
systematic relationship between the residuals and the ratio of heterotrophic and autotrophic taxa has been observed.
Since selective degradation plays at most a subordinate role in biasing dinocyst assemblages in this study and life-cycle factors
explain an independent dimension of the taxa variance, we consider the dinocyst assemblage compositions in the calibration
515 datasets as being mostly driven by environmental factors. However, most of the taxa variance in the local calibration dataset
cannot be explained even when all tested environmental factors (including water depth and distance from shore) are combined.
First, the combination of taxa to achieve higher consistency may hide a finer ecologically relevant taxonomic level. Since



studies revealed the existence of cryptic species in modern dinoflagellates (Montresor et al., 2003; Parkinson et al., 2016; Wang et al., 2019) and since some taxa are grouped voluntarily during analysis, finer relevant taxonomic levels are very likely. 520 It is, however, currently unavoidable because routine analyses (de Vernal et al., 2020) do not allow a refinement in regard to taxonomic levels.

Further, cyst-producing dinoflagellates lose their mobility at cyst formation, from which time onwards they are subject to ocean current transport until they reach the ocean floor. Although we excluded sample sides areas with strong oceanographic currents, small-size dinocyst particles might still be subject to transport by moderate currents when not incorporated in marine 525 snow or faecal pellets (e.g. Turner 2002, 2015) or bottom water currents and sediment flows (Dale, 1992; Dale and Dale, 1992). This may result in a lateral relocation and sedimentation from a cysts formation environment and thus in an additional nuisance in the calibration dataset (Nooteboom et al., 2019).

Additional noise may also emerge from modern assemblages in the calibration dataset, which represent average fluxes over different time intervals. Assemblages may be to a different degree affected by anthropogenic effects, such as local pollution 530 or global warming. Assemblages from sites with low sediment accumulation may represent averages over millennia and contain a mixture of microfossils deposited during distinct oceanographic events of the late Holocene (e.g. Wigley et al., 1981; Bradley and Jonest, 1993) or be affected by cysts deposited during conditions induced by modern anthropogenic global change. Alternatively, it is possible that the tested parameters are not the most determinant ones or that the assemblage composition is to a certain degree driven by biotic interactions rather than by environmental factors. It is also possible that environmental 535 factors, not yet considered, play an important role. These could include turbulence, micronutrients, stratification, or any other parameters that might be difficult to quantify for data treatment purposes.

Regardless of the limitations that can be due to missing or unidentified driving parameters, we find three mutually independent ecological gradients driving dinocyst assemblages in the local calibration dataset. This confirms previous findings that phytoplankton (Lopes et al., 2010) and hence dinocyst assemblages reflect multiple environmental drivers (e.g. Radi and de 540 Vernal, 2008; Ribeiro and Amorim, 2008; Hohmann et al., 2020).

The existence of multiple environmental gradients affecting the dinocyst assemblage composition implies that it should be possible to extract information from the same fossil dinocyst assemblage on past variability for more than one environmental driver. Whilst this is correct theoretically, one must consider the (small) amount of variance constrained by the tested parameters against the (large) portion of the variance that remains unconstrained. For example, primary productivity, which 545 represents the third gradient after SST and SSS, explains a maximum of 6 % of the constraint variability in the RDA (Table 6 and 7). This parameter does not contribute to the first two dimensions of the MFA and the RDA (see also Radi and de Vernal, 2008; de Vernal et al., 2020) and although the extracted relationship appears statistically significant, it may well be overwhelmed by factors that are responsible for the unconstrained portion of the variance in assemblage composition.

Additionally, we note that the presence of multiple environmental gradients in the local calibration dataset is associated with 550 spatial structuring of the environment (S6 – supplementary material). This may result in the fact that some environmental drivers deemed significant in the RDA, are only significant because they drive the taxa composition in a specific area with a



strong gradient of the given factor. This is in line with the observed spatial autocorrelation of the tested variables (S4 – supplementary material) and explains the performance decrease of MAT in the h-block cross-validation (Table 8) and as well as the strong spatial structure observed in the residuals of all methods (S6 – supplementary material). These observations are coherent with findings in Hohmann et al. (2020), where the observed multiple and mutually independent environmental factors driving the dinocyst assemblage composition in two larger regional datasets may be resulting from the agglomeration of information from regions with unlike environmental (primary) drivers and endemic taxon-environment relationships. To test this effect quantitatively, we performed a q-mode factor analysis for the local dataset, where taxa were clustered into factors to analyse interrelationships among their large number and to explain them in terms of their common underlying dimensions with respect to assemblage driving parameters. The information contained in individual taxa was condensed into a smaller set of information. We found that most taxa showed correlation coefficients < 0.3 with the retained factors, suggesting that driving parameters for taxa do not remain the same even throughout the region of the local Baffin Bay dataset. Hence, our results suggest even more localised driving mechanisms for dinocyst assemblage compositions in very specific areas. This implies that generating locally calibrated transfer functions will come at the cost of loss of generalisation and limited applicability to past oceanographic states.

Being based upon differing basic principles, the applied transfer function approaches seem to be affected differently by the detected local dataset's spatial structuring and the region-dependent primary drivers (Kucera et al., 2005). ML transfer functions appear to be unable to disclose and depict the taxon-environment relationship when multiple gradients affect the taxa assemblages (highest RMSEPs, lowest r^2 , fewest significant transfer functions). However, ML and WA-PLS performances are less affected by the effect of spatial autocorrelation. During h-block cross-validation, their performances remain similar, while the performances of MAT transfer functions plummet, returning higher RMSEP and lower r^2 than ML and WA-PLS (Table 8). On the other hand, performances of MAT based on LOO cross-validation are more optimistic than for ML and WA-PLS. While MAT finds the local structure in the assemblage data, ML and WA-PLS, which are based on a unimodal species-environment response model, find the general component of the variation in the assemblage data that is correlated with a specific environmental forcing. While all approaches have their advantages, ML and WA-PLS are more robust with regard to the detected spatial structure in the data than MAT (Telford and Birks, 2005). Cross-validation of the local dataset applying a calibration and verification dataset results in a 25 % lower $RMSEP_v$ for the verification dataset compared to the calibration dataset for SSSsummer, while $RMSEP_v$ are < 10 % lower for SSTsummer (2 %) and PPspring (8 %). This indicates that additional sample sites might benefit performances for SSSsummer transfer functions as with an adequate, hence representative, spatial coverage $RMSEP$ should be similar for both datasets (Table 8).

Regardless of the statistical approach, a theoretical high-performance transfer function for one of the independent driving variables for assemblage composition in the local calibration dataset does not necessarily produce a reliable reconstruction applied to fossil downcore dinocyst assemblages. This is because we can never be sure that the main drivers for past assemblages were identical in the modern calibration dataset. To assess if the main past drivers resemble the main modern



585 drivers, we compared the transfer function reconstructions to the major compositional trends in fossil dinocyst assemblages as revealed by multivariate analyses.

Across the four records throughout Baffin Bay, the main pattern of dinocyst assemblage change during the Holocene can be identified as two biofacies shifts occurring around 4.0 ka and 6.7 ka (Fig. 6 and 8) throughout the whole study area and one regime shift occurring in Baffin Bay and Disco Bay between 1.0 and 1.5 ka. Despite the presence of this clear pattern, most transfer functions based on the local ($n = 421$) and regional ($n = 1968$) data sets reconstruct modest changes close to uncertainty for SSTsummer, SSSsummer and PPSpring (Fig. 6), likely reflecting the difficulty in attributing the taxa assemblage change to specific factors. Alternatively, one may argue that we have not retained the correct determinant parameters during the manual forward selection. For example, the Holocene records could reflect changes that were due to large shifts in sea ice coverage. Indeed, during the selection process, the analysis suggested that SeaIce does not explain a separate dimension of variance in the taxa assemblages within the local Baffin Bay dataset (S3 – supplementary material), as it revealed high collinearity with SSTsummer (Fig. 3). This means that regionally SeaIce and SSTsummer explain a similar taxa variance and while reconstructing one, we reconstruct a mixture of both parameters. It is also possible that the parameterisation of sea ice cover used here is not ideal to describe the relationship with dinocyst assemblages. In the context of Baffin Bay, SSSsummer, which is the parameter that appears to be best reconstructed, is likely a reflection of the regional hydrography closely related to the sea ice cover that matters for productivity. Therefore, we can only conclude that the environmental regime shifts around 1.3 ka, 4.0 ka and 6.7 ka appear to be driven by changes in local hydrography that were associated with salinity changes but considering the magnitude of the salinity changes implied by the transfer functions, it is unlikely that the dinocyst composition responded to salinity directly.

605

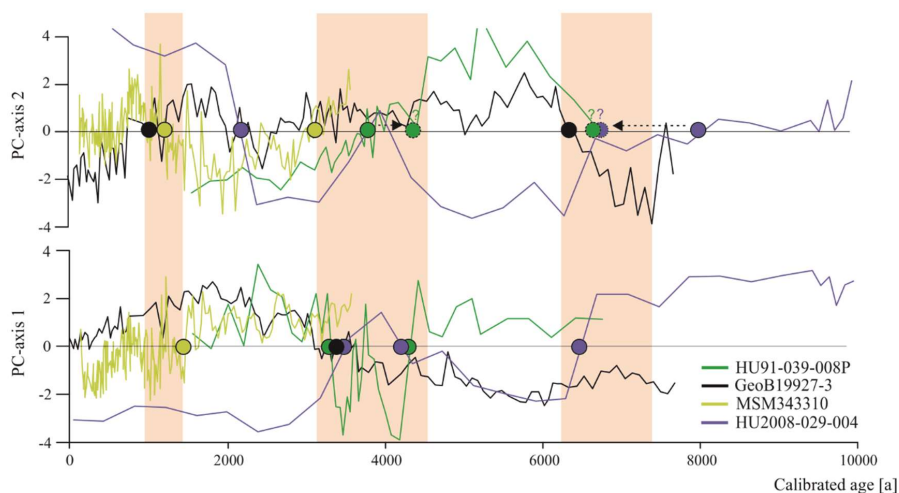


Figure 8: Dinocyst assemblage changes according to the first two PC-axes. Coloured dots represent PC transitions pointing to regime shifts around 1.3 ka (between 1.0 ka and 1.5 ka), 4.0 ka (between 3.1 ka and 4.3 ka) and 6.7 ka (orange shaded).

610

In contrast to the results of the local calibration, only a few of the reconstructions were identified as significant when applying the regional Northern Hemisphere dataset (SSTsummer = 16 %, SSSsummer = 25 %, PPspring = 8 %) (Table 9, Fig. 7). This suggests that transfer functions based on broad regional or even global calibration datasets are affected by nuisance variables, which makes it difficult to identify the driving mechanisms of dinocyst assemblages when the amplitude of environmental change is relatively small, as it is the case during the middle and late Holocene. For longer time intervals with large amplitude changes, global calibrations may work better and would be even necessary as larger datasets contain a wider range of analogues. Hence, we suggest a thorough evaluation of the calibration dataset and the significance of fossil applications ensuring that the driving mechanisms of dinocyst assemblages are caught through time and space.

615

620 4.2 Salinity reconstructions and regime shifts in the context of the existing regional paleoceanographic records

Results imply that in Baffin Bay most locally calibrated MAT and WA-PLS transfer functions produce robust Holocene reconstructions for summer salinity, being the main driver of dinocyst assemblage compositions while representing the regional hydrography closely related to sea ice cover and sea surface temperature driving the salinity changes. This poses the opportunity to interpret SSSsummer reconstructions within the context of the regional paleoceanography.



625 Until 7.6 ka Baffin Bay was still a region of extended sea ice and low primary productivity (e.g. Ouellet-Bernier et al., 2014; Jennings et al., 2014; Gibb et al., 2015; Caron et al., 2019; Limoges et al., 2020; Saini et al., 2020) (Fig. 9 d-g), while the Laurentide and the Greenland ice sheets continuously retreated (Fig. 9 a and b) (Dyke et al., 2003; Larsen et al., 2015). With the beginning of the Holocene Climate Optimum, sea ice cover in Baffin Bay retreated and it became a region of marginal ice zones until 6.3 ka. During this time, the first observed regime shift occurred between 7.6 ka and 6.3 ka (Fig.8) which is in accordance to the shift towards mild postglacial conditions in Baffin Bay proposed by Gibb et al. (2015) and Caron et al. (2019). In the northwest Labrador Sea (core HU2008-029-004) however, this postglacial transition already occurred around 11.9 ka (Gibb et al., 2015) implying that the observed regime shift also visible in both PCA-axes of HU2008-029-004, cannot - like in Baffin Bay - be ascribed to the postglacial transition.

630 After the transition phase from 6.3 ka on, salinity reconstructions propose a continuous increase in the northwest Labrador Sea and a continuous decrease of salinity in southern Melville Bay (Fig. 9 i and k). For Labrador Sea this is in accordance to findings in Gibb et al. (2015), who ascribes the increase to a reduction of stratification in the upper waters caused by the reduction of meltwater input from the Laurentide ice sheet and the increased advection of North Atlantic water (de Vernal et al., 2001; Solignac et al., 2004). Hence, the observed regime shift in the northwest Labrador Sea between 7.6 ka and 6.3 ka is in line with the suggested regional shift towards modern water circulation south of Davis Strait (Gibb et al., 2015).

640 For southern Melville Bay, other records also propose a slow salinity decrease between 5.5 ka and 1.4 ka (Gibb et al., 2015; Caron et al., 2019), which might be attributed to the still active process of postglacial meltwater discharge north of Davis Strait. This can be supported by a continuous decrease in sea ice cover in this region (Fig. 9 d-f; Gibb et al., 2015, Caron et al., 2019; Saini et al., 2020) and the increase in primary productivity after the first observed regime shift (e.g. Caron et al., 2019; Limoges et al., 2020). At the Southwest Greenland margin dinoflagellate blooms in summer-fall have been associated with freshwater inputs due to meltwater runoff from the GIS, which triggers upwelling of nutrient-rich waters and high productivity (Juul-Pedersen et al., 2015; Krawczyk et al., 2015, 2018). Along most of the West Greenland margin, sea-ice melt and meltwater runoff from the GIS result in seasonal stratification of surface waters, which is amplified in summer by solar heat leading to relatively mild conditions (Juul-Pedersen et al., 2015; Tremblay et al., 2015) also enhancing primary productivity. Pollen data indicate a high influx of long-distance pollen over Northwest Greenland during this time, indicating a milder climate (Funder, 1978; Fredskild, 1985; Fredskild and Andrews, 1985).

650 In northernmost Baffin Bay, our reconstructions show no general trend but a continuously oscillating salinity (Fig. 9 h), which is supported by reconstructions in Levac et al. (2001). Like in Levac et al. (2001), our reconstructed values stay below 32, indicating lower values than today's modern instrumental values.

However, while a general trend towards lower salinity can be observed north of Davis Strait and south of the northernmost Baffin Bay after 5.5 ka, other studies (Gibb et al., 2015; Caron et al., 2019) also find a salinity peak around 3.7 ka, interrupting the general trend, which is not visible in our reconstruction, although, this salinity peak corresponds to the second regime shift indicated by the PCA of all four studied cores (Fig. 8). This change in dinocyst assemblage compositions is also mentioned in Caron et al. (2019) for southern Melville Bay, although other dinocyst records from this region did not observe a shift (Ouellet-



Bernier et al., 2014; Gibb et al., 2015). In northernmost Baffin Bay, our reconstructions point to a period of slightly increased
660 salinity during the regime shift (Fig. 9 h). For the Baffin Bay area this shift may mark the final adaptation of assemblage
compositions to full interglacial conditions, supported by still continuously decreasing sea ice cover (Fig. 9) and other
paleoclimate studies along the southwest Greenland margin suggesting that optimum conditions were attained between 6.0 and
3.5 ka (Moros et al., 2006; Lloyd et al., 2007; Seidenkrantz et al., 2007; Ren et al., 2009; Andresen et al., 2010; Perner et al.,
2013).

665 In northernmost Baffin Bay and northwest Labrador Sea however, the changes in assemblage compositions are not stable,
changing again within the supposed period of the regime shift (Fig. 8). For northern Baffin Bay Levac et al. (2001) find a
general deterioration of sea surface conditions after 3.6 ka, which was accompanied by extensive sea ice cover. These findings
are supported by the second regime shift, implying changes in the dinocyst assemblage composition.

The late Holocene is locally characterized by the Neoglacial cooling trend (Weidick et al., 2012), which along the West
670 Greenland coast, is associated with subsurface cooling and glacier advances (e.g. Perner et al. 2013; Briner et al., 2016;
Schweinsberg et al., 2017) over the last 4.0 ka (e.g. Knudsen et al., 2008; Seidenkrantz et al., 2008; Krawczyk et al., 2010;
Andresen et al., 2010). This cooling trend is marked by climate oscillations, including the short warming phases of the Roman
Warm Period (2250-1600 years BP) (Lamb, 2002) and the Medieval Climatic Optimum (1100-700 years BP) (Lamb, 1965;
Mann, 2002). In Baffin Bay records, the trend's impact becomes visible from around 2.2 ka (Fig. 9). Regional cooling
675 accompanied by decreasing summer solar insolation (Berger and Loutre, 1991), fostering regrowth of the GIS (Briner et al.,
2010; Weidick and Bennike, 2007; Young et al., 2011), as well as cooling over the GIS (Dahl-Jensen et al., 1998) led to more
extensive sea ice, which was accompanied by increasing sea-surface salinity and a decline in primary productivity. Around
1.3 ka the southern Melville Bay core (GeoB19927-3) and the Disco Bay core (MSM343330) suggest a regime shift supporting
the assumption of a transition towards colder climate. This is also in accordance with proxy records from eastern Baffin Bay
680 suggesting glacier advances (Ouellet-Bernier et al., 2014; Gajewski, 2015) and decreased terrigenous detrital supply (Caron et
al., 2020) in this time interval.

Overall, the reconstructions for summer salinity and the observed regime shifts fit into and support the current picture of West
Greenland's paleoceanography. Comparing salinity reconstructions for southern Melville Bay (GeoB19927-3) with
reconstructions of sea ice cover from the same core derived from the biomarker proxy $P_{DIP_{25}}$ (Belt and Müller, 2013) for late-
685 spring sea ice cover (Saini et al., 2020), similar changes can be observed. Increasing sea ice cover correlates with increasing
salinity and vice versa. This additionally supports the significance of SSSsummer WA-PLS reconstructions in the Melville
Bay core and supports the assumption that salinity and sea ice cover are tightly coupled environmental drivers in this area.

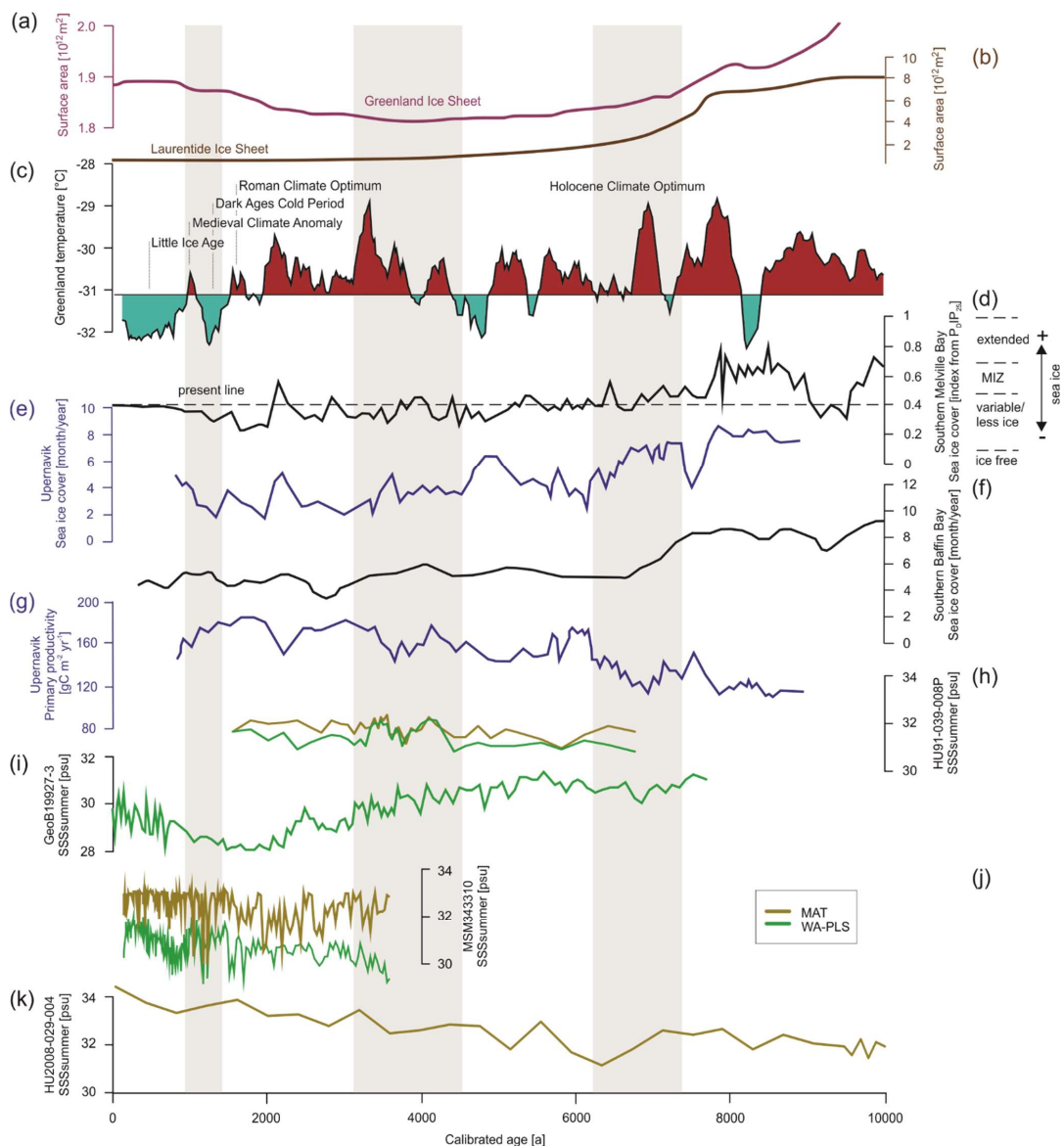


Figure 9: Time series for significant SSSsummer reconstructions (Table 9) (local MAT and WA-PLS) from the four studied cores

compared to different environmental records from the Baffin Bay region. (a) Greenland Ice Sheet area (Larsen et al., 2015), (b)

695 Laurentide Ice Sheet area (Dyke et al., 2003) (plots after Briner et al. (2016)), (c) Holocene Greenland temperatures based on $\delta^{18}\text{O}$ from the



GISP ice core (Alley et al., 2010), (d) sea ice cover in Southern Melville Bay based on biomarkers (Saini et al., 2020) (MIZ – marginal ice zone), (e) sea ice cover in Upernavik based on dinocyst assemblages (3-point running mean) (Caron et al., 2019), (f) sea ice cover in Southern Baffin Bay based on dinocyst assemblages (5-point running mean) (Gibb et al., 2015; Jennings et al., 2014), (g) primary productivity in Upernavik based on dinocyst assemblages (3-point running mean) (Caron et al., 2019), (h) SSSsummer from core HU91-039-008P, (i) SSSsummer from core GeoB19927-3, (j) SSSsummer from core MSM343310 and (k) SSSsummer from core HU2008-029-004. Regime shifts (Figure 8) are shaded in grey.

5 Conclusion

705 Understanding past natural variability of ecosystem drivers in Arctic regions requires reliable reconstructions. We calibrated local transfer functions from Baffin Bay samples for three independent parameters driving dinocyst assemblages in this area. We estimated how well these local functions were able to estimate past environmental parameters in the Baffin Bay region during the Holocene, comparing them to estimates derived from regional transfer functions from Northern Hemisphere samples and afterwards comparing the significant local transfer functions with the existing regional paleoceanographic records.

710 Statistical analyses of surface sediment samples and transfer function application on downcore samples from a Holocene transect along the Baffin Bay indicate that salinity is the main driver of present-day and Holocene dinocyst assemblage composition in the region, with temperature being an important but minor driver.

Analyses of four Holocene records in a North-South transect along the Baffin Bay show three regime shifts that occurred throughout the region. The main environmental parameter to which the dinoflagellate communities seem to have reacted during regime shifts is salinity, but further minor drivers may have differed regionally. The reconstructed salinity records and regime shifts support the current state of knowledge of West Greenland's Holocene paleoceanography.

715 We show that the relationship between dinocyst assemblage composition and multiple environmental drivers can be modelled by MAT and WA-PLS transfer functions. In our study, the identification of main driving variables and regime shifts was achieved through the application of a local calibration dataset, while through the application of the Northern Hemisphere dataset, we did not succeed in extracting this information from the taxa variability. While our results reinforce the assumption of counteracting nuisance in spatially large calibration datasets, suggesting the application of local datasets, regions with spatially or temporarily broader environmental gradients might supposedly benefit from larger calibration datasets regardless of a certain nuisance.

720 We suggest a thorough evaluation of transfer function performances and significances for downcore applications to disclose the specific drivers for present and fossil dinocyst assemblages in a studied core location. To this end, a local calibration dataset, which reduces several nuisances, is presumably beneficial when the amplitude of parameter change is relatively small, like during the middle and late Holocene.



Data availability

This study contains supplementary material. This material includes the matrices of taxa abundances with all tested
730 environmental (oceanographic and non-oceanographic) variables from the local $n = 421$ dataset (S1), DCA analysis plot (S2),
script of manual forward selection (S3), spatial autocorrelation analysis plots (S4), variogram plots for the estimation of h in
the h -block cross-validation (S5), residual plots from cross-validation tests (S6) and cross-correlation plots from
reconstructions (S7). The R codes applied for analyses and the script for manual forward selection (S3) can be accessed on
ZENODO (<https://doi.org/10.5281/zenodo.7773468>). Dinocyst assemblage data from the newly analysed core GeoB19927-3
735 (S1) are uploaded to PANGAEA and will be available soon.

Author contribution

All three (co-) authors collectively contributed to the conceptualisation of this study. Michal Kucera and Anne de Vernal
acquired funding and provided resources. Sabrina Hohmann developed the methodology with the supervision of Michal
740 Kucera, compiled the necessary data and performed all formal analyses. Visualisation of research results and original draft
preparation was done by Sabrina Hohmann. Michal Kucera and Anne de Vernal reviewed and edited the original draft.

Competing interests

The authors declare that they have no conflict of interest.

745 Acknowledgements

This study is a contribution of the International Research Training Group “Processes and Impacts of Climate Change in the
North Atlantic Ocean and the Canadian Arctic” (ArcTrain), which was supported jointly by the German Research Foundation
(DFG) (IRTG 1904) and by the Natural Sciences and Engineering Research Council of Canada (NSERC). We also
acknowledge the support from the Fonds de recherche du Québec – Nature et Technologie (FRQNT). We are grateful to
750 Taoufik Radi and Sebastien Zaragosi for their help in the preparation of the reference oceanographical data set and we
especially thank Maryse Henry for her extraordinary support during sample analyses.

References

Allan, E., de Vernal, A., Knudsen, M.F., Hillaire-Marcel, C.: Late Holocene sea-surface instabilities in the Disko Bugt area,



- west Greenland, in phase with d18O-oscillations at Camp Century, *Paleogeography and Paleoclimatology*, 33, 227-224,
755 <https://doi.org/10.1002/2017PA003289>, 2018.
- Alley, R.B., Andrews, J.T., Brigham-Grette, J., Clarke, G.K.C., Cuffey, K.M., Fitzpatrick, J.J., Funder, S., Marshall, S.J.,
Miller, G.H., Mitrovica, J.X., Muhs, D.R., Otto-Bliesner, B.L., Polyak, L., White, J.W.C.: History of the Greenland Ice
Sheet: paleoclimatic insights, *Quat. Sci. Rev.*, 29, 1728-1756, <https://doi.org/10.1016/j.quascirev.2010.02.007>, 2010.
- Andresen, C.S., Mccarthy, D.J., Dylmer, C.V., Seidenkrantz, M., Kuijpers, A., Lloyd, J.M.: Interaction between subsurface
760 ocean waters and calving of the Jakobshavn Isbræ during the late Holocene, *The Holocene*, 21, 211-224,
<https://doi.org/10.1177/0959683610378877>, 2010.
- Beamud, S.G., Diaz, M.M., Baccala, N.B., Pedrozo, F.L.: Limnological analysis of patterns of vertical and temporal distribution
of phytoplankton using multifactorial analysis: Acidic Lake Caviahue , Patagonia , Argentina, *Limnologia*, 40, 140–
147, <https://doi.org/10.1016/j.limno.2009.11.003>, 2010.
- 765 Belt, S.T., Müller, J.: The Arctic sea ice biomarker IP25: a review of current understanding, recommendations for future
research and applications in palaeo sea ice reconstructions, *Quat. Sci. Rev.*, 79, 9–25, <https://doi.org/10.1016/j.quascirev.2012.12.001>, 2013.
- Berger, A., Loutre, M.F.: Insolation values for the climate of the last 10 million years, *Quat. Sci. Rev.*, 10, 297–317, 1991.
- Berger, W.H., Smetacek, V., Wefer, G.: Ocean productivity and paleoproductivity - an overview, in: *Productivity of the Ocean:
770 Present and Past*, John Wiley & Sons Limited, 1–34, 1989.
- Birks, J.B.: Quantitative palaeoenvironmental reconstructions, in: *Statistical Modelling of Quaternary Science Data*, Maddy,
D., Brew, I.S. (Eds.), Quaternary Research Association, Cambridge, 271, 1995.
- Bradley, R.S., Jonest, P.D.: ' Little Ice Age ' summer temperature variations: their nature and relevance to recent global
warming trends, *Holocene*, 3, 367–376, <https://doi.org/10.1177/0959683693003000>, 1993.
- 775 Bravo, I., Figueroa, R.: Towards an ecological understanding of dinoflagellate cyst functions, *Microorganisms*, 2, 11–32,
<https://doi.org/10.3390/microorganisms2010011>, 2014.
- Briner, J.P., Stewart, H.A.M., Young, N.E., Philipps, W., Losee, S.: Using proglacial-threshold lakes to constrain fluctuations
of the Jakobshavn Isbræ ice margin, western Greenland, during the Holocene, *Quat. Sci. Rev.*, 29, 3861–3874,
<https://doi.org/10.1016/j.quascirev.2010.09.005>, 2010.
- 780 Briner, J.P., McKay, N.P., Axford, Y., Bennike, O., Bradley, R.S., de Vernal, A., Fisher, D., Francus, P., Fréchette, B.,
Gajewski, K., Jennings, A., Kaufman, D.S., Miller, G., Rouston, C., Wagner, B.: Holocene climate change in Arctic
Canada and Greenland, *Quat. Sci. Rev.*, 147, 340–364, <https://doi.org/10.1016/j.quascirev.2016.02.010>, 2016
- Burman, P., Bhow, E., Nonal, D.: A cross-validatory method for dependent data, *Biometrika*, 81, 351–358,
<https://doi.org/10.1093/biomet/81.2.351>, 1994.
- 785 Carlson, M.L., Flagstad, L.A., Gillet, F., Mitchell, E.A.D.: Community development along a proglacial chronosequence: are
above-ground and below-ground community structure controlled more by biotic than abiotic factors?, *J. Ecol.*, 98, 1084–
1095, <https://doi.org/10.1111/j.1365-2745.2010.01699.x>, 2010.



- Caron, M., Rochon, A., Carlos, J., Serrano, M., Onge, G.S.T.: Evolution of sea-surface conditions on the northwestern Greenland margin during the Holocene, *J. Quat. Sci.*, 34, 569–580, <https://doi.org/10.1002/jqs.3146>, 2019.
- 790 Caron, M., Montero-Serrano, J.C., St-Onge, G., Rochon, A.: Quantifying Provenance and Transport Pathways of Holocene Sediments From the Northwestern Greenland Margin, *Paleoceanogr. Paleoclimatology*, 35, 1–23, <https://doi.org/10.1029/2019PA003809>, 2020.
- Dahl-Jensen, D., Mosegaard, K., Gundestrup, N., Clow, G.D., Johnsen, S.J., Hansen, A.W., Balling, N.: Past Temperatures Directly from the Greenland Ice Sheet, *Science*, 282, 268–271, <https://doi.org/10.1126/science.282.5387.268>, 1998.
- 795 Dale, B.: *Dinoflagellate resting cysts: “benthic plankton,” survival strategies of the algae*, Cambridge University Press, 1983.
- Dale, B.: Dinoflagellate contributions to the open ocean sediment flux, in: *Dinoflagellate Contributions to the Deep Sea*, Dale, B., Dale, A.L. (Eds.), *Ocean Biocoenosis Ser.*, 1–31, 1992.
- Dale, B., Dale, A.L.: Dinoflagellate contributions to the sediment flux of the Nordic Seas, in: *Dinoflagellate Contributions to the Deep Sea*, Dale, B., Dale, A.L. (Eds.), *Ocean Biocoenosis Ser.*, 45–75, 1992.
- 800 Dale, B., Dale, A.L., Jansen, J.H.F.: Dinoflagellate cysts as environmental indicators in surface sediments from the Congo deep-sea fan and adjacent regions, *Palaeogeogr. Palaeoclimatol. Palaeoecol.*, 185, 309–338, [https://doi.org/10.1016/S0031-0182\(02\)00380-2](https://doi.org/10.1016/S0031-0182(02)00380-2), 2002.
- de Vernal, A., Marret, F.: Organic-walled dinoflagellate cysts: Tracers of sea-surface conditions, in: *Developments in Marine Geology*, Elsevier B.V., 371–408, [https://doi.org/10.1016/S1572-5480\(07\)01014-7](https://doi.org/10.1016/S1572-5480(07)01014-7), 2007.
- 805 de Vernal, A., Rochon, A., Turon, J.-L., Matthiessen, J.: Organic-walled dinoflagellate cysts: Palynological tracers of sea-surface conditions in middle to high latitude marine environments, *Geobios.*, 30, 905–920, [https://doi.org/10.1016/S0016-6995\(97\)80215-X](https://doi.org/10.1016/S0016-6995(97)80215-X), 1997.
- de Vernal, A., Hillaire-Marcel, C., Turon, J.-L., Matthiessen, J.: Reconstruction of sea-surface temperature, salinity, and sea-ice cover in the northern North Atlantic during the last glacial maximum based on dinocyst assemblages, *Can. J. Earth Sci.*, 37, 725–750, 2000.
- 810 de Vernal, A., Henry, M., Matthiessen, J., Mudie, P.J., Rochon, A., Boessenkool, K., Eynaud, F., Grøsfjeld, K., Guiot, J., Hamel, D., Harland, R., Head, M.J., Kunz-Pirrung, M., Levac, E., Loucheur, V., Peyron, O., Pospelova, V., Radi, T., Turon, J.-L., Voronina, E.: Dinoflagellate cyst assemblages as tracers of sea-surface conditions in the northern North Atlantic, Arctic and sub-Arctic seas: the new “n= 677” data base and its application for quantitative palaeoceanographic reconstruction, *J. Quat. Sci.*, 16, 681–698, <https://doi.org/10.1002/jqs.659>, 2001.
- 815 de Vernal, A., Eynaud, F., Henry, M., Hillaire-Marcel, C., Londeix, L., Mangin, S., Matthiessen, J., Marret, F., Radi, T., Rochon, A., Solignac, S., Turon, J.L.: Reconstruction of sea-surface conditions at middle to high latitudes of the Northern Hemisphere during the Last Glacial Maximum (LGM) based on dinoflagellate cyst assemblages, *Quat. Sci. Rev.*, 24, 897–924, <https://doi.org/10.1016/j.quascirev.2004.06.014>, 2005.
- 820 de Vernal, A., Henry, M., Bilodeau, G.: Micropaleontological preparation techniques and analyses, *Cahiers du Geotop*, 3, 2010.



- de Vernal, A., Rochon, A., Fréchette, B., Henry, M., Radi, T., Solignac, S.: Reconstructing past sea ice cover of the Northern Hemisphere from dinocyst assemblages: Status of the approach, *Quat. Sci. Rev.*, 79, 122–134, <https://doi.org/10.1016/j.quascirev.2013.06.022>, 2013.
- 825 de Vernal, A., Radi, T., Zaragosi, S., Van Nieuwenhove, N., Rochon, A., Allan, E., De Schepper, S., Eynaud, F., Head, M.J., Limoges, A., Londeix, L., Marret, F., Matthiessen, J., Penaud, A., Pospelova, V., Price, A., Richerol, T.: Percentages of common modern dinoflagellate cyst taxa in surface sediments of the Northern Hemisphere and corresponding environmental parameters, *PANGAEA*, <https://doi.org/10.1594/PANGAEA.908494>, 2019.
- 830 de Vernal, A., Radi, T., Zaragosi, S., Van Nieuwenhove, N., Rochon, A., Allan, E., De Schepper, S., Eynaud, F., Head, M.J., Limoges, A., Londeix, L., Marret, F., Matthiessen, J., Penaud, A., Pospelova, V., Price, A., Richerol, T.: Distribution of common modern dinoflagellate cyst taxa in surface sediments of the Northern Hemisphere in relation to environmental parameters: The new n=1968 database, *Mar. Micropaleontol.*, 159, 101796, <https://doi.org/10.1016/j.marmicro.2019.101796>, 2020.
- Dorschel, B., Afanasyeva, V., Bender, M., Dreutter, S., Eisermann, H., Gebhardt, A.C., Hansen, K., Hebbeln, D., Jackson, R.: 835 Past Greenland ice sheet dynamics, palaeoceanography and plankton ecology in the Northeast Baffin Bay - Cruise No. MSM44 “BAFFEAST” - June 30-July 30, 2015 - Nuuk (Greenland), *MARIA S. MERIAN-Berichte*, 51, https://doi.org/10.2312/cr_msm2344, 2015.
- Dray, S., Chessel, D., Thioulouse, J.: Co-inertia analysis and the linking of ecological data tables, *Ecology*, 84, 3078–3089, <https://doi.org/10.1890/03-0178>, 2003.
- 840 Dyke, A.S., Moore, A., Robertson, L.: Deglaciation of North America, *Geol. Surv. Can, Open File*, 2003.
- Efron, B., Gong, G.: A leisurely look at the bootstrap, the jackknife, and cross-validation, *Am. Stat.*, 37, 36–48, <https://doi.org/10.1080/00031305.1983.10483087>, 1983.
- Escofier, B., Pagès, J.: Analyse factorielle multiple, *Cah. du Bur. Univ. Rech. opérationnelle Série Rech.*, 42, 3–68, 1984.
- Escofier, B., Pagès, J.: Analyses factorielles simples et multiples: Objectifs, méthodes et interprétation, in: *Analyses 845 factorielles simples et multiples: Objectifs, méthodes et interprétation*, Dunod, Paris, 1990.
- Escofier, B., Pagès, J.: Multiple factor analysis (AFMULT package), *Comput. Stat. Data Anal.*, 18, 121–140, [https://doi.org/10.1016/0167-9473\(94\)90135-X](https://doi.org/10.1016/0167-9473(94)90135-X), 1994.
- Fensome, R.A., Taylor, F.J.R., Norris, G., Sarjeant, W.A.S., Wharton, D.I., Williams, G.L.: A classification of living and fossil dinoflagellates, *Micropaleontol. Spec. Pap.*, 7, 1–351, 1993.
- 850 Fischer, G., Ratmeyer, V., Wefer, G.: Organic carbon fluxes in the Atlantic and the Southern Ocean: Relationship to primary production compiled from satellite radiometer data, *Deep Sea Res. Part II Top. Stud. Oceanogr.*, 47, 1961–1997, [https://doi.org/10.1016/S0967-0645\(00\)00013-8](https://doi.org/10.1016/S0967-0645(00)00013-8), 2000.
- Fredskild, B.: The Holocene vegetational development of Tugtulligssuaq and Qeqertat, northwest Greenland, *Meddelelser om Grønland, Geoscience*, 14, 1–20, 1985.
- 855 Fredskild, B., Andrews, J.T.: Holocene pollen records from West Greenland, in: Andrews, J.T. (Ed.), *Quaternary*



- Environments: Eastern Canadian Arctic, Baffin Bay and Western Greenland, Allen and Unwin, Boston, 643–681, 1985.
- Funder, S.: Holocene (10,000-0 years BC) climates in Greenland, and North Atlantic atmospheric circulation, *Danish Meteorol. Inst. Climatol. Pap.*, 4, 175–181, 1978.
- Gajewski, K.: Quantitative reconstruction of Holocene temperatures across the Canadian Arctic and Greenland, *Glob. Planet. Change*, 128, 14–23, <https://doi.org/10.1016/j.gloplacha.2015.02.003>, 2015.
- 860 Gibb, O.T., Steinhauer, S., Frechette, B., de Vernal, A., Hillaire-Marcel, C.: Diachronous evolution of sea surface conditions in the Labrador Sea and Baffin Bay since the last deglaciation, *The Holocene*, 25, 1882–1897, <https://doi.org/10.1177/0959683615591352>, 2015.
- Guiot, J., Gally, Y.: R Package: bioindic, 2014.
- 865 Head, M.J.: Modern dinoflagellate cysts and their biological affinities, in: *Palynology: Principles and Applications*, Jansonius, J., McGregor, D.C. (Eds.), American Association of Stratigraphic Palynologists Foundation, 1197–1248, 1996.
- Hernández-Almeida, I., Cortese, G., Chen, M.-T., Kucera, M.: Environmental determinants of radiolarian assemblages in the western Pacific since the last deglaciation, *Paleoceanography*, 32, 830–847, <https://doi.org/10.1002/2017PA003159>, 2017.
- 870 Hohmann, S., Kucera, M., de Vernal, A.: Identifying the signature of sea-surface properties in dinocyst assemblages: Implications for quantitative palaeoceanographical reconstructions by transfer functions and analogue techniques, *Mar. Micropaleontol.*, 159, 101816, <https://doi.org/https://doi.org/10.1016/j.marmicro.2019.101816>, 2020.
- Holzwarth, U., Esper, O., Zonneveld, K.A.F.: Distribution of organic-walled dinoflagellate cysts in shelf surface sediments of the Benguela upwelling system in relationship to environmental conditions, *Mar. Micropaleontol.*, 64, 91–119, 875 <https://doi.org/10.1016/j.marmicro.2007.04.001>, 2007.
- Imbrie, J., Kipp, N.G.: A new micropaleontological method for quantitative paleoclimatology: Application to a late Pleistocene Caribbean core, in: *The Late Cenozoic Glacial Ages*, Turekian, K.K. (Ed.), Yale University Press, New Haven, 71–181, 1971.
- Jennings, A.E., Walton, M.E., Ó Cofaigh, C., Kilfeather, A., Andrews, J.T., Ortiz, J.D., De Vernal, A., Dowdeswell, J.A.: 880 Paleoenvironments during Younger Dryas-Early Holocene retreat of the Greenland Ice Sheet from outer Disko Trough, central west Greenland, *J. Quat. Sci.*, 29, 27–40, <https://doi.org/10.1002/jqs.2652>, 2014.
- Josse, J., Pagès, J., Husson, F.: Testing the significance of the RV coefficient, *Comput. Stat. Data Anal.*, 53, 82–91, <https://doi.org/10.1016/j.csda.2008.06.012>, 2008.
- Juggins, S.: *Rioja: Analysis of Quaternary science data*, 2017.
- 885 Juul-Pedersen, T., Arendt, K.E., Mortensen, J., Blicher, M.E., Søgaard, D.H., Rysgaard, S.: Seasonal and interannual phytoplankton production in a sub-Arctic tidewater outlet glacier fjord, SW Greenland, *Mar. Ecol. Prog. Ser.*, 524, 27–38, <https://doi.org/10.3354/meps11174>, 2015.
- Kassambara, A., Mundt, F.: *Factoextra: Extract and visualize the results of multivariate data analyses*, R package version, 1, 2017.



- 890 Kaufman, D., McKay, N., Routsos, C., Erb, M., Dätwyler, C., Sommer, P.S., Heiri, O., Davis, B.: Holocene global mean surface temperature, a multi-method reconstruction approach, *Sci. Data*, 7, 201, <https://doi.org/10.1038/s41597-020-0530-7>, 2020.
- Knudsen, K.L., Stabell, B., Seidenkrantz, M.S., Eiríksson, J., Blake, W.: Deglacial and Holocene conditions in northernmost Baffin Bay: Sediments, foraminifera, diatoms and stable isotopes, *Boreas*, 37, 346–376, <https://doi.org/10.1111/j.1502-3885.2008.00035.x>, 2008.
- 895 Koc, N., Jansen, E., Hafliðason, H.: Paleocceanographic reconstruction of surface ocean conditions in the Greenland, Iceland, and Norwegian seas through the last 14,000 years based on diatoms, *Quat. Sci. Rev.*, 12, 115–140, [https://doi.org/10.1016/0277-3791\(93\)90012-B](https://doi.org/10.1016/0277-3791(93)90012-B), 1993.
- Kokinos, J.P., Eglinton, T.I., Gon, M.A.: Characterization of a highly resistant biomacromolecular material in the cell wall of a marine dinoflagellate resting cyst, *Organic*, 28, 265–288, [https://doi.org/10.1016/S0146-6380\(97\)00134-4](https://doi.org/10.1016/S0146-6380(97)00134-4), 1998.
- 900 Krawczyk, D., Witkowski, A., Moros, M., Lloyd, J., Kuijpers, A., Kierzek, A.: Late-Holocene diatom-inferred reconstruction of temperature variations of the West Greenland Current from Disko Bugt, Central West Greenland, *The Holocene*, 20, 659–666, <https://doi.org/10.1177/0959683610371993>, 2010.
- Krawczyk, D.W., Witkowski, A., Juul-Pedersen, T., Arendt, K.E., Mortensen, J., Rysgaard, S.: Microplankton succession in a SW Greenland tidewater glacial fjord influenced by coastal inflows and run-off from the Greenland Ice Sheet, *Polar Biol.*, 38, 1515–1533, <https://doi.org/10.1007/s00300-015-1715-y>, 2015.
- 905 Krawczyk, D.W., Meire, L., Lopes, C., Juul-Pedersen, T., Mortensen, J., Li, C.L., Krogh, T.: Seasonal succession, distribution, and diversity of planktonic protists in relation to hydrography of the Godthåbsfjord system (SW Greenland), *Polar Biol.*, 41, 2033–2052, <https://doi.org/10.1007/s00300-018-2343-0>, 2018.
- 910 Kucera, M., Weinelt, M., Kiefer, T., Pflaumann, U., Hayes, A., Weinelt, M., Martin, M., Mix, A.C., Barrows, T.T., Cortijo, E., Duprat, J., Juggins, S., Waelbroeck, C.: Reconstruction of sea-surface temperatures from assemblages of planktonic foraminifera: multi-technique approach based on geographically constrained calibration data sets and its application to glacial Atlantic and Pacific Oceans, *Quat. Sci. Rev.*, 24, 951–998, <https://doi.org/10.1016/j.quascirev.2004.07.014>, 2005.
- 915 Lamb, H.H.: The early medieval warm epoch and its sequel, *Palaeogeogr. Palaeoclimatol. Palaeoecol.*, 1, 13–37, [https://doi.org/10.1016/0031-0182\(65\)90004-0](https://doi.org/10.1016/0031-0182(65)90004-0), 1965.
- Lamb, H.H.: *Climate, history and the modern world*, Routledge, 2002.
- Lamentowicz, M., Lamentowicz, Ł., van der Knaap, W.O., Gabka, M., Mitchell, E.A.D.: Contrasting species-environment relationships in communities of testate amoebae, bryophytes and vascular plants along the Fen-Bog gradient, *Environ. Microbiol.*, 59, 499–510, <https://doi.org/10.1007/s00248-009-9617-6>, 2010.
- 920 Larsen, N.K., Kjær, K.H., Lecavalier, B., Bjørk, A.A., Colding, S., Huybrechts, P., Jakobsen, K.E., Kjeldsen, K.K., Knudsen, K.-L., Odgaard, B.V., Olsen, J.: The response of the southern Greenland ice sheet to the Holocene thermal maximum, *Geology*, 43, 291–294, 2015.



- Lê, S., Josse, J., Husson, F.: FactoMineR: An R package for multivariate analysis, *J. Stat. Softw.*, 25, 1–18, 925 <https://doi.org/10.18637/jss.v025.i01>, 2008.
- Legendre, P., Gallagher, E.D.: Ecologically meaningful transformations for ordination of species data, *Oecologia*, 129, 271–280, <https://doi.org/10.1007/s004420100716>, 2001.
- Lepš, J., Šmilauer, P. (Eds.): *Multivariate analysis of ecological data using CANOCO*, Cambridge university press, 2003.
- Levac, E., De Vernal, A., Blake, W.: Sea-surface conditions in northernmost Baffin Bay during the Holocene: Palynological 930 evidence, *J. Quat. Sci.*, 16, 353–363, <https://doi.org/10.1002/jqs.614>, 2001.
- Limoges, A., Weckström, K., Ribeiro, S., Georgiadis, E., Hansen, K.E., Martinez, P., Seidenkrantz, M.S., Giraudeau, J., Cros-
ta, X., Massé, G.: Learning from the past: Impact of the Arctic Oscillation on sea ice and marine productivity off north-
west Greenland over the last 9,000 years, *Glob. Chang. Biol.*, 26, 6767–6786, <https://doi.org/10.1111/gcb.15334>, 2020.
- Lloyd, J.M., Kuijpers, A., Long, A., Moros, M., Park, L.A.: Foraminiferal reconstruction of mid- to late-Holocene ocean 935 circulation and climate variability in Disko Bugt, West Greenland, *The Holocene*, 17, 1079–1091, <https://doi.org/10.1177/0959683607082548>, 2007.
- Lopes, C., Mix, A.C., Abrantes, F.: Environmental controls of diatom species in northeast Pacific sediments, *Palaeogeogr. Palaeoclimatol. Palaeoecol.*, 297, 188–200, <https://doi.org/10.1016/j.palaeo.2010.07.029>, 2010.
- Mann, M.E.: Medieval Climatic Optimum. *Encycl. Glob. Environ. Chang.*, 1, 514–516, 2002.
- 940 Marcott, S.A., Shakun, J.D., Clark, P.U., Mix, A.C.: A Reconstruction of regional and global temperature for the past 11,300 years, *Science*, 339, 1198–1201, <https://doi.org/10.1126/science.1228026>, 2013.
- Marret, F.: Les effets de l’acétylolyse sur les assemblages de kystes de dinoflagelle’s, *Palynosciences*, 2, 267–272, 1993.
- Matthiessen, J.: Distribution patterns of dinoflagellate cysts and other organic-walled microfossils in recent Norwegian-Greenland Sea sediments, *Mar. Micropaleontol.*, 24, 307–334, [https://doi.org/10.1016/0377-8398\(94\)00016-G](https://doi.org/10.1016/0377-8398(94)00016-G), 1995.
- 945 Matthiessen, J., Baumann, K.H., Schröder-Ritzrau, A., Hass, C., Andruleit, H., Baumann, A., Jensen, S., Kohly, A., Pflaumann, U., Samtleben, C., Schäfer, P., Thiede, J.: Distribution of calcareous, siliceous and organic-walled planktic microfossils in surface sediments of the Nordic Seas and their relation to surface-water masses, in: *The Northern North Atlantic*, Schäfer, P., Ritzrau, W., Schlüter, M., Thiede, J. (Eds.), Springer, Berlin Heidelberg, 105–127, https://doi.org/10.1007/978-3-642-56876-3_7, 2001.
- 950 McGarigal, K., Stafford, S., Cushman, S.: Discriminant analysis, in: *Multivariate statistics for wildlife and ecology research*, Springer, New York, 129–187, https://doi.org/10.1007/978-1-4612-1288-1_4, 2000.
- Meyers, P.A.: Organic geochemical proxies of paleoceanographic, paleolimnologic, and paleoclimatic processes, *Org. Geochem.*, 27, 213–250, [https://doi.org/https://doi.org/10.1016/S0146-6380\(97\)00049-1](https://doi.org/https://doi.org/10.1016/S0146-6380(97)00049-1), 1997.
- Montresor, M., Sgroso, S., Procaccini, G., Wiebe, H.C.F.: Intraspecific diversity in *Scrippsiella trochoidea* (Dinophyceae): 955 evidence for cryptic species, *Phycologia*, 42, 56–70, <https://doi.org/10.2216/i0031-8884-42-1-56.1>, 2003.
- Morey, A.E., Mix, A.C., Pisias, N.G.: Planktonic foraminiferal assemblages preserved in surface sediments correspond to multiple environment variables, *Quat. Sci. Rev.*, 24, 925–950, <https://doi.org/10.1016/j.quascirev.2003.09.011>, 2005.



- Moros, M., Jensen, K.G., Kuijpers, A.: Mid- to late-Holocene hydrological and climatic variability in Disko Bugt, central West Greenland, *The Holocene*, 16, 357–367, <https://doi.org/10.1191/0959683606hl933rp>, 2006.
- 960 Mudie, P.J.: Circum-Arctic Quaternary and Neogene marine palynofloras: paleoecology and statistical analysis, *Neogene Quat. Dinoflag. cysts acritarchs*, 10, 347–390, 1992.
- Muller, P.J., Erlenkeuser, H., Von Grafenstein, R.: Glacial-interglacial cycles in oceanic productivity inferred from organic carbon contents in eastern north Atlantic sediment cores, in: *Coastal upwelling, its sediment record, part B: Sedimentary records of ancient coastal upwelling*, Thiede J., Suess, E. (Ed.), Plenum Press, New York, 65–398, 1983.
- 965 Nootboom, P.D., Bijl, P.K., Sebille, E. Van, Heydt, A.S. Von Der, Dijkstra, H.A.: Transport bias by ocean currents in sedimentary microplankton assemblages: Implications for paleoceanographic reconstructions, *Paleogeography and Paleoclimatology*, 34, 1178–1194, <https://doi.org/10.1029/2019PA003606>, 2019.
- Nychka, D., Furrer, R., Sain, S.: fields: Tools for spatial data, <https://doi.org/10.5065/D6W957CT>, 2017.
- Oksanen, J., Blanchet, F.G., Friendly, M., Kindt, R., Legendre, P., McGlinn, D., Minchin, P.R., O’Hara, R.B., Simpson, G.L., 970 Solymos, P., Stevens, M.H.H., Szoecs, E., Wagner, H.: *Vegan: Community ecology package (version 2.5-6)*, The Comprehensive R Archive Network, 2019.
- Ouellet-Bernier, M.M., de Vernal, A., Hillaire-Marcel, C., Moros, M.: Paleoceanographic changes in the Disko Bugt area, West Greenland, during the Holocene, *Holocene*, 24, 1573–1583, <https://doi.org/10.1177/0959683614544060>, 2014.
- Parkinson, J.E., Baumgarten, S., Michell, C.T., Baums, I.B., Lajeunesse, T.C., Voolstra, C.R.: Gene expression variation 975 resolves species and individual strains among coral-associated dinoflagellates within the genus *Symbiodinium*, *Genome Biol. Evol.*, 8, 665–680, <https://doi.org/10.1093/gbe/evw019>, 2016.
- Pebesma, E.J.: Multivariable geostatistics in S: the gstat package, *Comput. Geosci*, 30, 683–691, <https://doi.org/10.1016/j.cageo.2004.03.012>, 2004.
- Pebesma, E.J., Bivand, R.S.: S classes and methods for spatial data: the sp package, *R news*, 5, 9–13, 2005.
- 980 Perner, K., Moros, M., Jennings, A.E., Lloyd, J.M., Knudsen, K.L.: Holocene palaeoceanographic evolution off West Greenland, *The Holocene*, 23, 374–387, <https://doi.org/10.1177/0959683612460785>, 2013.
- Price, A.M., Pospelova, V., Coffin, M.R.S., Latimer, J.S., Chmura, G.L.: Biogeography of dinoflagellate cysts in northwest Atlantic estuaries, *Ecol. Evol.*, 6, 5648–5662, <https://doi.org/10.1002/ece3.2262>, 2016.
- Price, A.M., Baustian, M.M., Turner, R.E., Rabalais, N.N., Chmura, G.L.: Dinoflagellate cysts track eutrophication in the 985 Northern Gulf of Mexico, *Estuaries and Coasts*, 41, 1322–1336, <https://doi.org/10.1007/s12237-017-0351-x>, 2018.
- R Core Team: *R: A language and environment for statistical computing*, 2017.
- Radi, T., de Vernal, A.: Dinocyst distribution in surface sediments from the northeastern Pacific margin (40–60°N) in relation to hydrographic conditions, productivity and upwelling, *Rev. Palaeobot. Palynol.*, 128, 169–193, [https://doi.org/10.1016/S0034-6667\(03\)00118-0](https://doi.org/10.1016/S0034-6667(03)00118-0), 2004.
- 990 Radi, T., de Vernal, A.: Dinocysts as proxy of primary productivity in mid-high latitudes of the Northern Hemisphere, *Mar. Micropaleontol.*, 68, 84–114, <https://doi.org/10.1016/j.marmicro.2008.01.012>, 2008.



- Radi, T., de Vernal, A., Peyron, O.: Relationships between dinoflagellate cyst assemblages in surface sediment and hydrographic conditions in the Bering and Chukchi seas, *J. Quat. Sci.*, 16, 667–680, <https://doi.org/10.1002/jqs.652>, 2001.
- 995 Rao, C.R.: A review of canonical coordinates and an alternative to correspondence analysis using Hellinger distance, *Qüestiió*, 19, 23–63, 1995.
- Ren, J., Jiang, H., Seidenkrantz, M.S., Kuijpers, A.: A diatom-based reconstruction of Early Holocene hydrographic and climatic change in a southwest Greenland fjord, *Mar. Micropaleontol.*, 70, 166–176, <https://doi.org/10.1016/j.marmicro.2008.12.003>, 2009.
- 1000 Ribeiro, S., Amorim, A.: Environmental drivers of temporal succession in recent dinoflagellate cyst assemblages from a coastal site in the North-East Atlantic (Lisbon Bay, Portugal), *Mar. Micropaleontol.*, 68, 156–178, <https://doi.org/10.1016/j.marmicro.2008.01.013>, 2008.
- Robert, P., Escoufier, Y.: A unifying tool for linear multivariate statistical methods: The RV-coefficient, *Appl. Stat.*, 25, 257–265, <https://doi.org/10.2307/2347233>, 1976.
- 1005 Rochon, A., de Vernal, A.: Palynomorph distribution in recent sediments from the Labrador Sea, *Can. J. Earth Sci.*, 31, 115–127, <https://doi.org/10.1139/e94-010>, 1994.
- Rochon, A., de Vernal, A., Turon, J.-L., Matthießen, J., Head, M.J.: Distribution of recent dinoflagellate cysts in surface sediments from the North Atlantic Ocean and adjacent seas in relation to sea-surface, *Am. Assoc. Stratigr. Palynol. Contrib. Ser.*, 35, 1–164, <https://doi.org/10013/epic.14283>, 1999.
- 1010 Rochon, A., Eynaud, F., de Vernal, A.: Dinocysts as tracers of hydrographical conditions and productivity along the ocean margins: Introduction, *Mar. Micropaleontol.*, 68, 1–5, <https://doi.org/10.1016/j.marmicro.2008.04.001>, 2008.
- Rühlemann, C., Müller, P.J., Schneider, R.R.: Organic carbon and carbonate as paleoproductivity proxies: Examples from high and low productivity areas of the tropical Atlantic, in: *Use of proxies in paleoceanography: Examples from the South Atlantic*, Fischer, G., Wefer, G. (Eds.), Springer, Berlin Heidelberg, 315–344, https://doi.org/10.1007/978-3-642-58646-0_12, 1999.
- 1015 Saini, J., Stein, R., Fahl, K., Weiser, J., Hebbeln, D., Hillaire, C., de Vernal, A.: Holocene variability in sea ice and primary productivity in the northeastern Baffin Bay, *Arktos*, <https://doi.org/10.1007/s41063-020-00075-y>, 2020.
- Sarnthein, M., Winn, K., Duplessy, J.-C., Fontugne, M.R.: Global variations of surface ocean productivity in low and mid latitudes: Influence on CO₂ reservoirs of the deep ocean and atmosphere during the last 21,000 years, *Paleoceanography*, 3, 361–399, <https://doi.org/10.1029/PA003i003p00361>, 1988.
- 1020 Schlitzer, R.: *Ocean Data View*, odv.awi.de, 2018.
- Schröder-Adams, C.J., van Rooyen, D.: Response of recent benthic foraminiferal assemblages to contrasting environments in Baffin Bay and the northern Labrador Sea, *Northwest Atlantic, Arctic*, 64, 317–341, <https://doi.org/10.14430/arctic4122>, 2011.
- 1025 Schweinsberg, A.D., Briner, J.P., Miller, G.H., Bennike, O., Thomas, E.K.: Local glaciation in West Greenland linked to North



- Atlantic ocean circulation during the Holocene, *Geology*, 45, 195–198, <https://doi.org/10.1130/G38114.1>, 2017.
- Seidenkrantz, M.S., Aagaard-Sørensen, S., Sulsbrück, H., Kuijpers, A., Jensen, K.G., Kunzendorf, H.: Hydrography and climate of the last 4400 years in a SW Greenland fjord: Implications for Labrador Sea palaeoceanography, *Holocene*, 17, 387–401, <https://doi.org/10.1177/0959683607075840>, 2007.
- 1030 Seidenkrantz, M.S., Roncaglia, L., Fischel, A., Heilmann-Clausen, C., Kuijpers, A., Moros, M.: Variable North Atlantic climate seesaw patterns documented by a late Holocene marine record from Disko Bugt, West Greenland, *Mar. Micropaleontol.*, 68, 66–83, <https://doi.org/10.1016/j.marmicro.2008.01.006>, 2008.
- Sha, L., Jiang, H., Seidenkrantz, M.S., Knudsen, K.L., Olsen, J., Kuijpers, A., Liu, Y.: A diatom-based sea-ice reconstruction for the Vaigat Strait (Disko Bugt, West Greenland) over the last 5000 yr, *Palaeogeogr. Palaeoclimatol. Palaeoecol.*, 403, 1035 66–79, <https://doi.org/10.1016/j.palaeo.2014.03.028>, 2014.
- Solignac, S., de Vernal, A., Hillaire-Marcel, C.: Holocene sea-surface conditions in the North Atlantic - Contrasted trends and regimes in the western and eastern sectors (Labrador Sea vs. Iceland Basin), *Quat. Sci. Rev.*, 23, 319–334, <https://doi.org/10.1016/j.quascirev.2003.06.003>, 2004.
- Taylor, F.J.R., Pollinger, U.: The ecology of dinoflagellate, in: *The biology of dinoflagellates*, Taylor, F.J.R. (Ed.), Blackwell Scientific Publications, Oxford, 398–529, 1987.
- 1040 Telford, R.J.: palaeoSig: Significance tests of quantitative palaeoenvironmental reconstructions, R package version, 1, 2015.
- Telford, R.J., Birks, H.J.B.: The secret assumption of transfer functions: Problems with spatial autocorrelation in evaluating model performance, *Quat. Sci. Rev.*, 24, 2173–2179, <https://doi.org/10.1016/j.quascirev.2005.05.001>, 2005.
- Telford, R.J., Birks, H.J.B.: Evaluation of transfer functions in spatially structured environments, *Quat. Sci. Rev.*, 28, 1309–1045 1316, <https://doi.org/10.1016/j.quascirev.2008.12.020>, 2009.
- Telford, R.J., Birks, H.J.B.: A novel method for assessing the statistical significance of quantitative reconstructions inferred from biotic assemblages, *Quat. Sci. Rev.*, 30, 1272–1278, <https://doi.org/10.1016/j.quascirev.2011.03.002>, 2011.
- ter Braak, C.J.F.: Canonical correspondence analysis: A new eigenvector technique for multivariate direct gradient analysis, *Ecology*, 67, 1167–1179, <https://doi.org/10.2307/1938672>, 1986.
- 1050 ter Braak, C.J.F.: Ordination, in: *Data analysis in community and landscape ecology*, Jongman, R.H., ter Braak, C.J.F., van Tongeren, O.F.R. (Eds.), Center for Agricultural Publishing and Documentation, Wageningen, The Netherlands, 91–169, 1987.
- Trachsel, M., Telford, R.J.: Technical note: Estimating unbiased transfer-function performances in spatially structured environments, *Clim. Past*, 12, 1215–1223, <https://doi.org/10.5194/cp-12-1215-2016>, 2016.
- 1055 Tremblay, J.É., Anderson, L.G., Matrai, P., Coupel, P., Bélanger, S., Michel, C., Reigstad, M.: Global and regional drivers of nutrient supply, primary production and CO₂ drawdown in the changing Arctic Ocean, *Prog. Oceanogr.*, 139, 171–196, <https://doi.org/10.1016/j.pocean.2015.08.009>, 2015.
- Turner, J.T.: Zooplankton fecal pellets, marine snow, phytodetritus and the ocean’s biological pump, *Prog. Oceanogr.*, 130, 205–248, <https://doi.org/10.1016/j.pocean.2014.08.005>, 2015.



- 1060 Turner, J.T.: Zooplankton fecal pellets, marine snow and sinking phytoplankton blooms, *Aquat. Microb. Ecol.*, 27, 57–102, <https://doi.org/10.3354/ame027057>, 2002.
- van Nieuwenhove, N., Head, M.J., Limoges, A., Pospelova, V., Mertens, K.N., Matthiessen, J., De Schepper, S., de Vernal, A., Eynaud, F., Londeix, L., Marret, F., Penaud, A., Radi, T., Rochon, A.: An overview and brief description of common marine organic-walled dinoflagellate cyst taxa occurring in surface sediments of the Northern Hemisphere, *Mar. Micropaleontol.*, 159, 101814, <https://doi.org/10.1016/j.marmicro.2019.101814>, 2020.
- 1065 Wall, D., Dale, B.: Modern dinoflagellate cysts and evolution of the Peridinales, *Micropaleontology*, 14, 265–304, 1968.
- Wang, N., Mertens, K.N., Krock, B., Luo, Z., Derrien, A., Pospelova, V., Liang, Y., Bilién, G., Smith, K.F., De Schepper, S., Wietkamp, S., Tillmann, U., Gu, H.: Cryptic speciation in *Protoceratium reticulatum* (Dinophyceae): Evidence from morphological, molecular and ecophysiological data, *Harmful Algae*, 88, 101610, <https://doi.org/10.1016/j.hal.2019.05.003>, 2019.
- 1070 Weidick, A., Bennike, O.: Quaternary glaciation history and glaciology of Jakobshavn Isbræ and the Disko Bugt region, West Greenland: A review, *Geological Survey of Denmark and Greenland Bulletin*, <https://doi.org/10.34194/geusb.v14.4985>, 2007.
- Weidick, A., Bennike, O., Citterio, M., Nørgaard-Pedersen, N.: Neoglacial and historical glacier changes around Kangersuneq fjord in southern West Greenland, *Geological Survey of Denmark and Greenland Bulletin*, <https://doi.org/10.34194/geusb.v27.4694>, 2012.
- 1075 Wigley, T.M.L., Ingram, M.J., Farmer, G.: Past climates and their impact on man: A review, in: *Climate and History*, Cambridge University Press, New York, 3–50, 1981.
- Young, N.E., Briner, J.P., Stewart, H.A.M., Axford, Y., Csatho, B., Rood, D.H., Finkel, R.C.: Response of Jakobshavn Isbræ, Greenland, to Holocene climate change, *Geology*, 39, 131–134, <https://doi.org/10.1130/G31399.1>, 2011.
- 1080 Zamelczyk, K., Rasmussen, T.L., Husum, K., Haflidason, H., de Vernal, A., Ravna, E.K., Hald, M., Hillaire-Marcel, C.: Paleooceanographic changes and calcium carbonate dissolution in the central Fram Strait during the last 20 ka, *Quat. Res.*, 78, 405–416, <https://doi.org/10.1016/j.yqres.2012.07.006>, 2012.
- Zonneveld, K.A.F., Siccha, M.: Dinoflagellate cyst based modern analogue technique at test - A 300 year record from the Gulf of Taranto (Eastern Mediterranean), *Palaeogeogr. Palaeoclimatol. Palaeoecol.*, 450, 17–37, <https://doi.org/10.1016/j.palaeo.2016.02.045>, 2016.
- 1085 Zonneveld, K.A.F., Versteegh, G.J.M., de Lange, G.J.: Preservation of organic-walled dinoflagellate cysts in different oxygen regimes: a 10,000 year natural experiment, *Mar. Micropaleontol.*, 29, 393–405, [https://doi.org/10.1016/S0377-8398\(96\)00032-1](https://doi.org/10.1016/S0377-8398(96)00032-1), 1997.
- 1090 Zonneveld, K.A.F., Versteegh, G., Kodrans-Nsiah, M.: Preservation and organic chemistry of Late Cenozoic organic-walled dinoflagellate cysts: A review, *Mar. Micropaleontol.*, 68, 179–197, <https://doi.org/10.1016/j.marmicro.2008.01.015>, 2008.
- Zonneveld, K.A.F., Versteegh, G.J.M., Kasten, S., Eglinton, T.I., Emeis, K., Huguet, C., Koch, B.P.: Selective preservation of



organic matter in marine environments; processes and impact on the sedimentary record, *Biogeosciences*, 7, 483–511,
1095 <https://doi.org/10.5194/bg-7-483-2010>, 2010.

Zonneveld, K.A.F., Gray, D., Kuhn, G., Versteegh, G.J.M.: Postdepositional aerobic and anaerobic particulate organic matter
degradation succession reflected by dinoflagellate cysts: The Madeira Abyssal Plain revisited, *Mar. Geol.*, 408, 87–109,
<https://doi.org/10.1016/j.margeo.2018.11.010>, 2019.

1100

1105

1110

1115

1120